CORRELATION OF SEISMIC SECTION WITH GEOLOGIC BOREHOLE LOGS IN SOME STUDENT HOSTELS AT AHMADU BELLO UNIVERSITY (MAIN CAMPUS), ZARIA, KADUNA STATE.

BY

OSUMEJE JOSEPH OROJAH
M.Sc/SCI/45523/04-05

A RESEARCH THESIS SUBMITTED TO THE POSTGRADUATE SCHOOL, AHMADU BELLO UNIVERSITY, ZARIA, IN PARTIAL FULFILLMENT OF THE REQUIREMENTS FOR THE AWARD OF MASTERS DEGREE IN APPLIED GEOPHYSICS,

DEPARTMENT OF PHYSICS.
FACULTY OF SCIENCE,
AHMADU BELLO UNIVERSITY, ZARIA,

MARCH, 2008

DEDICATION

This work is dedicated to the Almighty God for his guidance and protection throughout the duration of this programme. To my unborn children.

DECLARATION

I hereby declare that, this thesis is an original work carried out by the author under the supervision of **Prof. I. B. Osazuwa (FNIP) and Dr P. Sule.** The information derived from the literature has been duly acknowledged in the text and a list of references provided. To the best of my knowledge, no part thereof has been submitted elsewhere for the award of degree. The works of others are duly acknowledged and referenced.

OSUMEJE JOSEPH OROJAH
Author

01/04/2008
Signature & Date

CERTIFICATION

This thesis entitled "CORRELATION OF SEISMIC SECTION WITH GEOLOGIC BOREHOLE LOGS IN SOME STUDENT HOSTELS AT AHMADU BELLO UNIVERSITY (MAIN CAMPUS), ZARIA, KADUNA STATE" by OSUMEJE Joseph Orojah, meets the regulations governing the award of the degree of Master of Science (Applied Geophysics) of Ahmadu Bello University Zaria and is approved for its contribution to knowledge and literary presentation

Prof. I. B. Osazuwa
Chairman Supervisory Committee.

01-04-2008
Date

Dr P. Sule
Member, Supervisory Committee

1/4/08
Date

Dr. N. Rabiu
Ag. Head of Department of physics

Date

Prof. S. A. Nkom
Dean, Postgraduate School.

Date

ACKNOWLEDGEMENT

My profound gratitude goes to GOD Almighty for his divine guardian and protection throughout my master programme.

Thanks to my supervisors, Prof. I. B. Osazuwa (FNIP) and Dr. P. O. Sule. I appreciate your efforts for finding time to go through this work despite your busy schedule.

I also want to in a special way thank Prof. I. B. Osazuwa through whom financial grants and equipment donated by the International Program in the Physical Sciences (IPPS), Uppsala University, Sweden was made available to me. This greatly enhanced the completion of this work. Sir, I appreciate you and the almighty God bless you.

My appreciation goes to all the staff of the Department of Physics, A. B. U., Zaria who have contributed in building me up academically. I thank Engr. A. C. Bamgbelu for all his Fatherly advice and moral support rendered to me.

I thank my lovely parents Mr. and Mrs. R. Osumeje for their endless care, advice and support towards my completion of this programme and to my brothers and sisters, Margaret, Thomas, Hellen, Blessing, Godwin, Patrick, Vickky, I am proud of you all.

I wish to specifically express my profound and sincere gratitude to a number of people who have motivated me through this programme; Onje A, Ebenezer K. Adaji U, Ivy M., Emmanuel O., Kate I., Innocent O., Chiemeke C., and my entire Geophysics course mate, I am indebted to you all. For all those whose names are not remembered, I appreciate you all.

ABSTRACT

Ahmadu Bcllo University is located in Zaria in the north-central part of the Nigerian basement complex. Zaria is situated in the Sudan Savannah area of the country. The aim of this Geophysical survey is to investigate the subsurface structure of the earth around some student hostels in the main campus of the university by correlating a borehole log with a generated seismic section. The objectives include; the determination of the nature and texture of the strata underlying the hostel buildings, the determination of the depth to fresh basement and the determination of the topography of the basement. Seismic refraction tomography methods was used for this investigation. A total of eight profiles were taken around four hostels, with the boreholes at the centre of the each spread. A total of about 120m spread was laid in a straight line with each geophone placed at 5m interval. The seismic data collected were processed using the REFLEX W software. From the processed data, the result shows a depth to fresh basement at about 24m deep around the survey area, which is undulating. The subsurface varies in texture from line to medium and coarse grain size, with clay dominating the weathered basement. This gives reason for the sinking and cracking of some structures within the survey area.

TABLE OF CONTENTS

Title	*Page*
Title Page	(i)
Dedication	(ii)
Declaration	(iii)
Certification	(iv)
Acknowledgement	(v)
Abstract	(vi)
Table of Content	(vii)
List of Figures	(xi)
List of Tables	(xiii)
CHAPTER ONE	
GENERAL OVERVIEW	1
1.1 General Introduction	1
1.2 Location and Description of Study Area	2
1.3 Geology of the Study Area	3
1.3.1 Crystalline Complex	5
1.3.2 The Metasediments	6
1.3.3 The Schist	6
1.3.4 Quartzites	6
1.3.5 Granitic Rocks	6
1.4 Previous works in the area	7
1.5 Aims and objectives of the Present Work	8

CHAPTER TWO

PRINCIPLES AND THEORIES OF SEISMIC METHOD 9

2.1 Seismic Waves 9

2.1.1 Seismic Body Waves 9

(i) Compressional or P Waves 10

(ii) Transverse Waves 11

2.1.2 Seismic Surface Waves 12

(i) Rayleigh waves 12

(ii) Love waves 13

2.2 Reflection and Refraction surveying 14

2.3 Seismic Reflection Method 16

2.3.1 Geometry of Reflection Wave Path 18

2.3.2 Dipping horizontal reflector 21

2.3.3 Ray paths of multiple reflections 23

2.4 Seismic Refraction Method 23

2.4.1 Geometry of Refracted Ray Path 28

2.4.2 Two-layer case with horizontal interface 28

2.4.3 Three-layer case with horizontal interfaces 30

2.4.4 Dipping layer case with planar interface 31

2.5 Elevation and Weathering Corrections 33

2.6 Refraction Tomography 33

CHAPTER THREE

INSTRUMENTATION AND FIELD PROCEDURE 36

3.1 Instrumentations 36

3.2 Preliminary Preparation 40

3.3 Testing of the Equipment 41

3.4 Factors to be considered for Field use 43
(i) Quality control 45
(ii) Noise 45
3.5 Field Procedure 46
3.6 Problems encountered on the field 47
3.7 Data collection 47
3.7.1 Precautions taken to ensure good results 48
(a) Observation of traffic and movement within the survey area 48
(b) Placement of geophones 48
(c) Placement of the trigger geophone 48
(d) Problem of offset 48

CHAPTER FOUR

DATA PROCESSING AND INTERPRETATION 49
4.1 Introduction 49
4.2 Processing of Seismic Tomography Data 50
4.2.1 Filtering 51
4.2.2 Picking of First Arrivals 52
4.2.3 Assigning the picked travel time into layer 53
4.3 Performing the Refraction Tomography 54
4.4 Interpretation 55
4.4.1 *Data Interpretation* 55
4.5 Interpretation of the Tomography Section 64

CHAPTER FIVE

SUMMARY, CONCLUSION AND RECOMMENDATION 83
5.1 Summary of Results 83

5.2 Conclusion 84

5.3 Recommendations 84

REFERENCES 85

LIST OF FIGURES

Figure 1.1:	Location of the study area	3
Figure 1.2:	Simplified Geologic Map of Nigeria	4
Figure 1.3:	Simplified basement geologic map of the Kubanni River, Zaria.	5
Figure 2.1:	The particle motion of a Rayleigh wave	13
Figure 2.2:	Travel-Time curve for direct, reflected and refracted rays	15
Figure 2.3:	The split-spread method for reflection method	18
Figure 2.4:	The geometry of reflected ray path for a horizontal reflector	19
Figure 2.5:	The geometry of reflected ray path for a dipping horizontal reflector	22
Figure 2.6:	Field layout of a seismograph showing path way of direct and refracted waves for a two-layer soil/ rock system.	26
Figure 2.7:	The direct and refracted waves through a two-layer model	27
Figure 2.8:	Travel –time curve for direct and refracted waves	28
Figure 2.9:	The refracted ray path for a three –layer model	30
Figure 2.10:	Travel-time curve and ray path for a dipping refractor	31
Figure 2.11:	Forward and reverse travel-time curve for Tomography data	35
Figure 3.1:	The measured menu	38
Figure 3.2:	The view data menu	39
Figure 3.3:	Seismograph Abem Terraloc MK6	42
Figure 3.4:	A typical Seismic wave from a single geophone	44
Figure 4.1:	Travel-time curve for profile 1	57
Figure 4.2:	Travel-time curve for profile 2	58
Figure 4.3:	Travel-time curve for profile 3	59
Figure 4.4:	Travel-time curve for profile 4	60

KADUNA POLYTECHNIC LIBRARY

Figure 4.5: Travel-time curve for profile 5 61

Figure 4.6: Travel-time curve for profile 6 62

Figure 4.7: Travel-time curve for profile 7 63

Figure 4.8: Travel-time curve for profile 8 64

Figure 4.9: Tomographic section of profile 1 - Akenzua Hostel 66

Figure 4.10: Tomographic section of profile 2 - Akenzua Hostel 68

Figure 4.11: Tomographic section of profile 3 - Amina Hostel 70

Figure 4.12: Tomographic section of profile 4 - Amina Hostel 72

Figure 4.13: Tomographic section of profile 5 - Ribadu Hostel 74

Figure 4.14: Tomographic section of profile 6 - Ribadu Hostel 76

Figure 4.15: Tomographic section of profile 7 - Suleiman Hostel 78

Figure 4.16: Tomographic section of profile 8 - Suleiman Hostel 80

LIST OF TABLES

Table 2.1:	Compressional wave velocities in Earth materials	24
Table 4.1:	Lithology, Aquifer and Geologic section of Borehole log 1	67
Table 4.2:	Lithology, Aquifer and Geologic section of Borehole log 2	69
Table 4.3:	Lithology, Aquifer and Geologic section of Borehole log 3	71
Table 4.4:	Lithology, Aquifer and Geologic section of Borehole log 4	73
Table 4.5:	Lithology, Aquifer and Geologic section of Borehole log 5	75
Table 4.6:	Lithology, Aquifer and Geologic section of Borehole log 6	77
Table 4.7:	Lithology, Aquifer and Geologic section of Borehole log 7	79
Table 4.8:	Lithology, Aquifer and Geologic section of Borehole log 8	81
Table 4.9:	Standard Velocity, Standard density and Tomography velocity	82

CHAPTER ONE

GENERAL OVERVIEW

1.1 Introduction

Seismic tomography signifies a revolution in earth sciences. It has had far-reaching and deep impacts on the geological and the geophysical community and will continue to influence the future developments in earth sciences. A seismic tomography image (analogous to the computer aided tomography scan, used in the medical industry) has been particularly useful in understanding the earth's structure and processes in the source zones of large earthquakes. Once an earthquake occurs, it generates seismic waves that pass through the earth's interior and finally arrive at the earth's surface, where they are recorded by seismographs. Analyses of the observed seismic waves provide information on the rupture process of the earthquake as well as physical properties of the materials along the wave trajectories. The classical studies on seismic waves had led to the discoveries of the layered structure of the earth and the advent of seismic tomography two decades ago had helped in the mapping of the heterogeneous structure of the earth on a broad range of scales. With the present acceleration in the development of seismic tomography, it is expected to be the most active field of seismological research.

Although, there are varieties of seismic techniques, the objective of a survey will determine which specific method to use. In refraction and reflection seismology, the arrival time of seismic energy that is refracted or reflected by the discontinuities between different rock formations are detected at a number of points by sensitive instruments called geophones. Knowing the distance travelled by the wave and time spent, it is possible to

determine the depth to the discontinuity, the velocities of the waves, the structural dip, and the lithology within the trajectory path in the earth.

1.2 Location of the Study Area

The study sites are located at Ahmadu Bello University main campus in Zaria, as shown in figure 1.1. Zaria is a town in Kaduna State (see Figure 1.1); located on a plateau at a height of about 760 m above the sea level. The main campus (ABU) which is about 15.5km from the well-known Zaria City is approximately bounded by longitude $7^{0}38^{1}$E and $7^{0}39^{1}$E and latitude $11^{0}09^{1}$N and $11^{0}10^{1}$N. We investigated the northern part of the main campus, which includes Akenzua Hall, Amina Hall, Alexander and Ribadu Halls and Suleiman Hall.

1.3 Geology of the study area

Ahmadu Bello University is a part of the gently undulating peneplain that extends from Lake Chad to Sokoto and Northward from Southern Kaduna into the Republic of Niger. Zaria is underlain by Precambrian rocks typical of Nigeria basement complex, (figure 1.2) which bear the imprint of thermo tectonic event dating from Achaean to early Paleozoic times (McCurry, 1970).

The main campus (Ahmadu Bello University) is underlain by Precambrian rocks of the basement complex (figure 1.1) with muscovite biotite-gneiss in the south-western part of the campus while the north-eastern part is underlain by biotite granite-gneiss (Eigbefo, 1978).

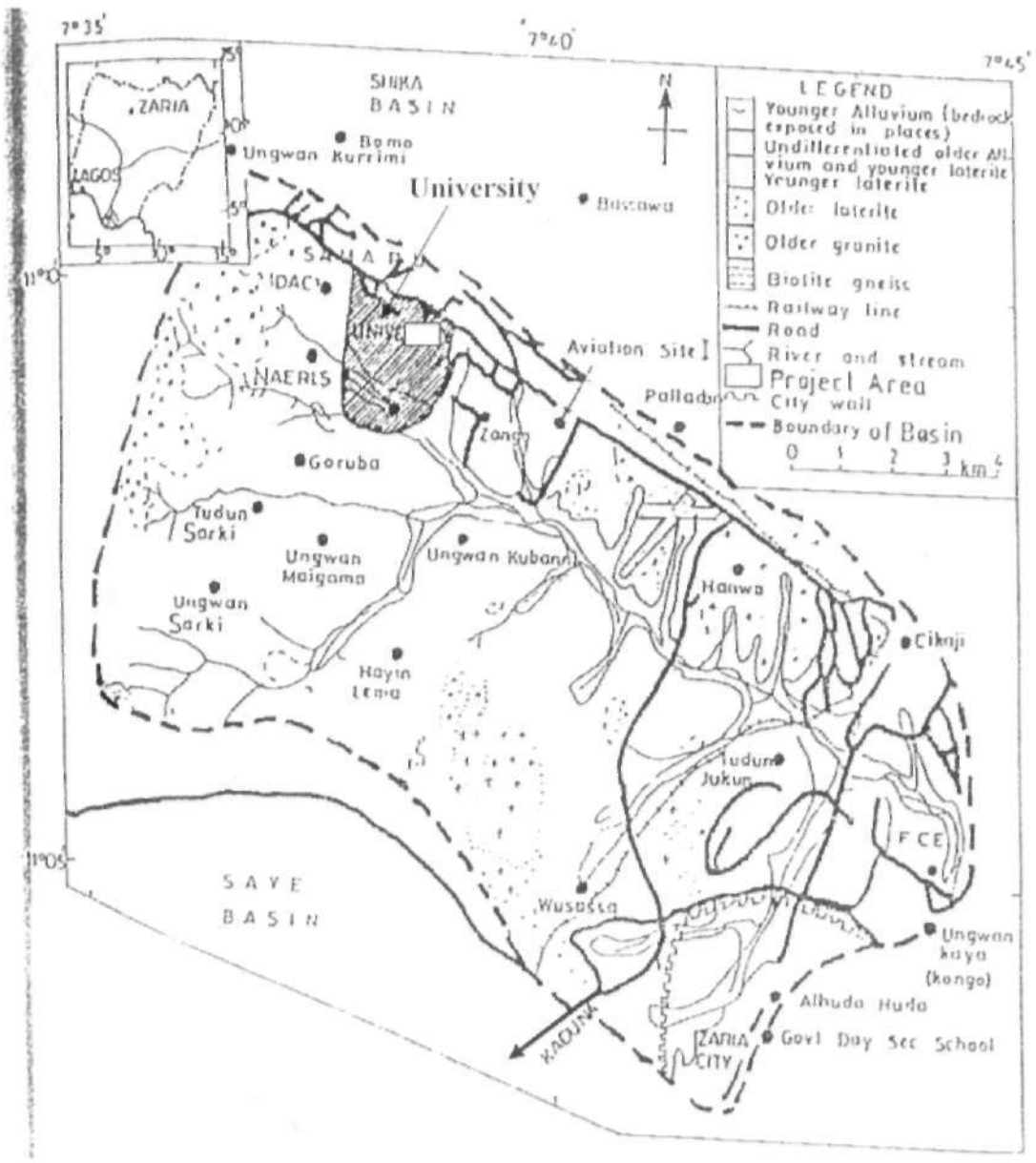


Figure 1.1: Location of the Study area (Ahmadu Bello University, Zaria. Main campus)

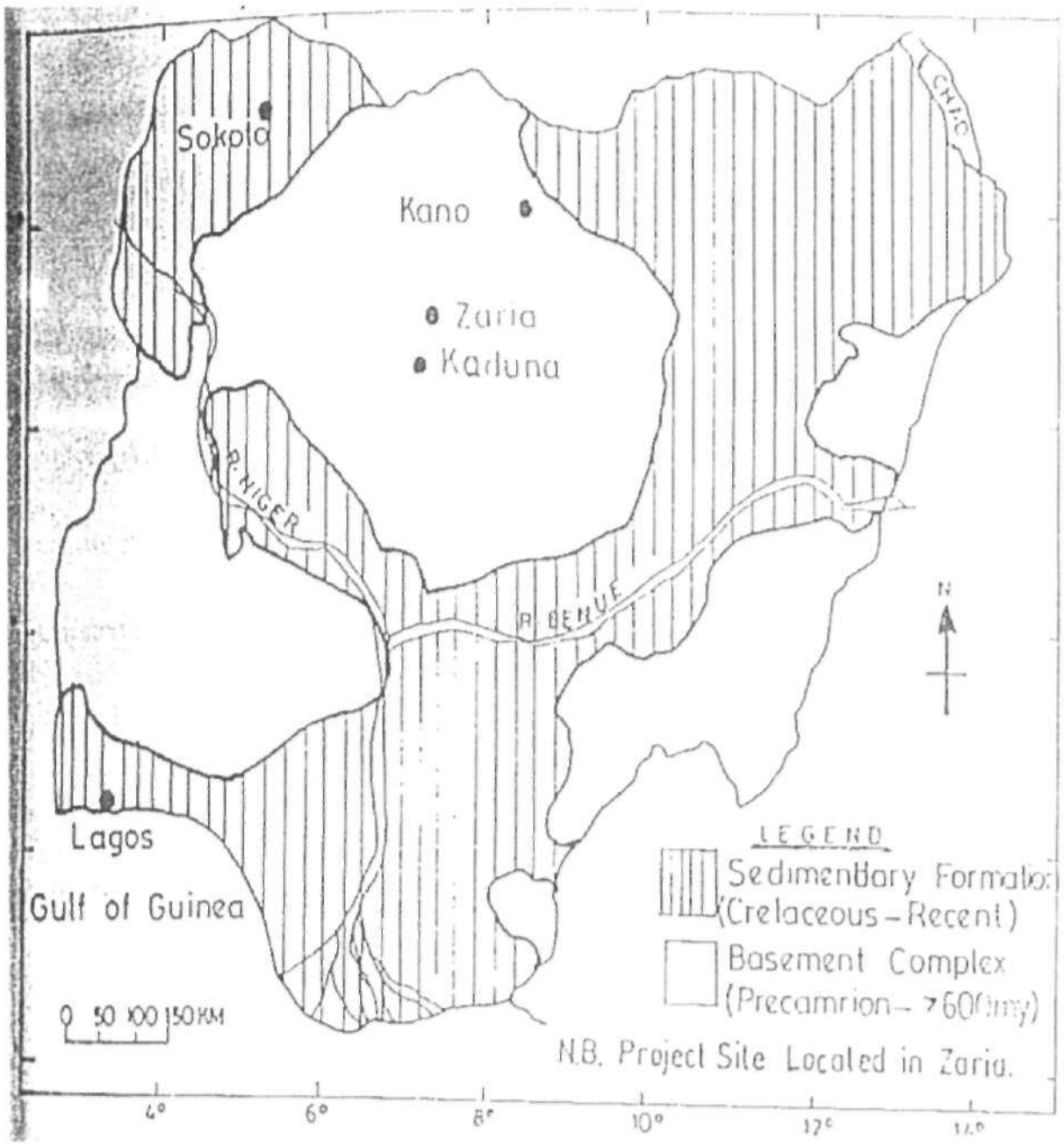


Figure 1.2: Simplified Geologic Map of Nigeria (after G.S.N. 1970)

The rocks in this area can be divided according to (McCurry, 1970) into:

(i) a crystalline complex of migmatite and gneisses probably of Dahomeyan age, including relics of an ancient Birrimian metasediment sequence,

(ii) a younger metasediment series of Katangan age occupying north-south trending synclinal belts in the crystalline complex, and

(iii) A suite of intrusive syntectonic to late tectonic granites and granodiorites of the late Precambrian to lower Paleozoic age associated with extensive aplite and pegmatite development.

These rocks have been variably metamorphosed and granitized through at least two tectono-metamorphic cycles and folded during the Pan African orogeny resulting in tight isoclinal folding about East-West and North-South axes and the alternating and deformation of rocks from low grade phyllites to high grade gneisses (McCurry, 1970). The geology of the study area can further be discussed under the following sub titles.

1.3.1 Crystalline Complex

Zaria area is underlain by ancient crystalline basement complex, which comprises gneisses and migmatites and also accommodates the belt of younger metasediments as well as remnants of an older metasedimentary group preserved mainly as feldspathic quartzites, amphibolites and calcareous rocks. The gneisses are very variable in composition including the biotite gneisses, the hornblende gneisses, banded gneisses, granite gneisses, sheared gneisses, augen gneisses and cataclastic gneisses. There is evidence that some of the gneisses are sedimentary in origin.

1.3.2. The Metasediments

These occur in north-south trending synclinal belts as lenses, which apparently have conformable relationships with the crystalline host-rock. The main subdivisions are the schists and quarzites.

1.3.3. Schists

These occupy the greater part of the metasediment belts and vary in colour, texture and outcrop. Due to their soft and friable nature, they are usually only exposed in river valleys and excavations where they are deeply weathered. Schists grade into adjacent crystalline gneisses. The various schists are muscovite-quartz schists, biotite-muscovite schists, feldspathic schists and carbonaceous schists.

1.3.4. Quartzites

The quartzites are well foliated especially the fissile varieties. Massive quartzites contain relatively few impurities and are usually grey-white in colour, while fissile varieties vary from yellow to brown depending on relative amount of muscovite and oxide present.

1.3.5. Granitic Rocks

These are well exposed especially in the Northwest area where extensive outcrops occur. Elsewhere, the granites are beneath a thick superficial cover, and only outcrop in isolated hills or groups of inselbergs, low whalebacks and granite pavements. The granite bodies range in size from sub-elliptical plutons not more than about 125 sq. km. in area up to masses of batholithic dimensions and fall into two groups:

KASHIM IBRAHIM LIBRARY

i. Elongate batholiths, discordant in part but mainly concordant, with rather diffuse contacts
ii. Discordant, much fractured bodies including crystalline rocks and metasediments with cross-cutting contacts.

The rocks are all compositionally similar in that they contain quartz, microcline, plagioclase and biotite as essential minerals, with accessory apatite and zircon. The different types of granitic rocks are porphyroblastic biotite granite, fine to medium-grained biotite granites, porphyroblastic hornblende granite and granodiorites.

Fine grained granites, aplites and pegmatites occur as irregular facies in the main granite bodies and in some of the surrounding gneisses. Also, these form concordant or discordant veins, lenses, pods and sheets and are particularly concentrated in the more richly porphyroblastic granites in the south-eastern part of the area (McCurry, 1970).

1.4 Previous Works in the Area

Although not much work on Seismic Tomography has been done on these part of the campus, however, Yusuf (2000) carried out a geoelectric investigation employing vertical electrical sounding (VES) to correlate the Ajayi Makinde two-electrode method and the conventional Schlumberger configuration. He revealed that the study area varies from 3-4 layers. The geometry of the bedrock undulates with varying depth of 11.5m in the central part of the campus to 30.0m around the southern part of the campus.

Chiemeke (2005) carried out a seismic tomography work around the Basawa military barracks, which is about 4km to 5km away from this study area. He was able to conclude that the tomography model showed a good correlation with the borehole log cited around the survey area by bringing out the three major layers (top soil, weathered basement and

fresh basement). His correlation was done using seismic velocities which agree with standard velocity values.

Ogah (1990) carried out the application of beam forming techniques to enhance low quality seismic refraction data at the Kubanni drainage basin. He came to the conclusion that the beam forming techniques represented a powerful and viable method of extracting useful information from low quality seismic refraction record.

1.5 Aims and Objective of the Present Work

The Ahmadu Bello University is a highly built up area with structures standing for over 4 to 5 decades. Most of these structures were erected without proper geophysical studies in the area for engineering construction, which results in the sinking and deformation of some of these structures. Geophysical investigation around these sites of visible deformations can provide possible solution to this problem. The above-mentioned problems have engendered this research work whose aim is to:

(a) Estimate the depth to the basement (overburden thickness).
(b) Estimate thickness of the weathered layer.
(c) Determine the lithology within the subsurface under investigation based on the physical parameter measured.
(d) Determine possible fracture zones.
(e) Determine depth of water table.
(f) Determine bedrock morphology.

KASHIM IBRAHIM LIBRARY

CHAPTER TWO

PRINCIPLES AND THEORY OF SEISMIC METHODS

2.1 Seismic waves

Seismic waves are short-lived parcels of elastic strain energy known as pulses that propagate from a source point through the Earth containing a wide range of frequency. The propagation of seismic disturbance through a heterogeneous medium is extremely complex although it can be described by some equations by making some simple assumptions. It is important to know that the strains (elastic displacements) due to the passage of these pulses are minute except for the source environment. However, when a seismic disturbance has travelled some distance away from its source, it attenuates and the medium deforms elastically to permit its passage. The particles of the medium carry out simple harmonic motions, and the seismic energy is transmitted as a series of wave motions. This implies that the propagating velocities of the seismic pulse are determined by the elastic moduli and density of the materials through which they pass.

When seismic energy is released suddenly at a point near the surface of a homogeneous medium, part of the energy propagates through the body of the medium, as seismic body waves. The remaining part of the energy, analogous to the ripples on the surface of a pool of water into which a stone has been thrown, propagates close to the surface as surface waves (Kearey et al., 2002). There are basically two types of seismic waves, body waves and surface waves.

2.1.1 Seismic Body Waves

Two types of body waves can be propagated within a medium. The first type, is known as a dilatational (longitudinal, compressional or P wave), the later name is due to the fact that

this wave is the first (primary) event on an earthquake recording. The second type is referred to as shear (transverse, rotational or S wave) since it is usually the second event observed on earthquake record.

(i) **Compressional (P) Waves:-** are compressional waves which have longitudinal particle motion aligned with the propagation direction. The deformation produced by the passage of these waves involves change in the volume of a material element and is directly analogous to the propagation of sound wave in a fluid. They travel faster in materials and are slightly less than twice as fast as Secondary (S) waves and can travel through any type of material, so the P-wave is the first-arriving energy on a seismogram. Generally has higher frequency than the Secondary (S) waves and Surface-waves. In air, these pressure waves take the form of sound waves; hence they travel at the speed of sound. Typical speeds are 330 m/s in air, 1450 m/s in water and about 5000 m/s in granite (the P-wave velocity (V_P) is about 5 km/s to 7 km/s in typical Earth's crust; greater than about 8 km/s in Earth's mantle and core; about 1.5 km/s in water; about 0.3 km/s in air). P waves are sometimes called "primary waves", and are not as destructive as the S waves and surface waves that follow them.

The property of this wave can be developed in terms of the equations of motion for an elastic solid and the relation between stress and strain. In terms of the bulk modulus k, the shear modulus μ, and the density ρ, the speed of propagation for the compressional wave is given as;

$$\alpha = \sqrt{\frac{k + \frac{4}{3}\mu}{\rho}} \qquad (2.1)$$

KASHIM IBRAHIM LIBRARY

Equation (2.1) shows that P-wave can travel through solids, liquids and gases, all of which are compressible. Liquids and gases do not allow shear waves to propagate through them. Consequently, when $\mu = 0$, and the compressional wave velocity in a fluid is given by

$$(\alpha)_{\mu=0} = \sqrt{\frac{k}{\rho}} \tag{2.2}$$

(ii) Transverse (S) Waves:- which are also known as secondary or shear waves induce shearing deformation with no change in volume, the particle motion is transverse to the propagation path (as in electromagnetic waves). *S* waves do not propagate through perfect fluids because they cannot sustain shear. Secondary waves travel slower than P-waves in a solid and, therefore, arrive after the P wave. The S-wave velocity (V_S) about 3 km/s to 4 km/s in typical Earth's crust; greater than about 4.5 km/s in Earth's mantle and about 2.5 km/s to 3.0 km/s in (solid) inner core.

The property of this wave can also be developed in terms of the equations of motion for an elastic solid and the relation between stress and strain. In terms of the shear modulus μ, and the density ρ, the speed of propagation for the transverse wave is given as;

$$\beta = \sqrt{\frac{\mu}{\rho}} \tag{2.3}$$

The only elastic property that determines the velocity of the shear waves is the rigidity or shear modulus (μ). In liquids and gases, if μ is zero, transverse waves cannot propagate in them, (Lowrie, 1997).

2.1.2 Seismic Surface Waves

They are analogous to water waves and travel just under the Earth's surface. They travel more slowly than body waves. Because of their low frequency, long duration, and large amplitude, they can be the most destructive type of seismic waves. The two types of surface waves: Rayleigh waves and Love waves are distinguished from each other by the type of particle motion in their wavefronts.

(i) **Rayleigh (R) Waves:-** also known as long waves or ground roll, travels on the surface of the Earth like water ripples. The existence of these waves was predicted by John William Strutt, Lord Rayleigh, in 1885. They are slower than body waves and can readily be seen during an earthquake on an open space like a parking lot where the cars move up and down with the waves. Rayleigh waves are also dispersive and the amplitudes generally decrease with depth in the Earth. Appearance and particle motion are similar to water waves; the resulting particle motion can be regarded as a combination of P and SV vibrations. Depth of penetration of the Rayleigh waves is also dependent on frequency, with lower frequencies penetrating to greater depth. Motion is both in the direction of propagation and perpendicular (in a vertical plane), and "phased" so that the motion is generally elliptical–either prograde or retrograde (figure 2.1). Rayleigh Waves speed (V_R) is about 2.0 km/s to 4.2 km/s (i.e. 0.9194 times the speed of Secondary Wave) in the Earth which depends on frequency of the propagating wave and the depth of penetration of the waves (Lowrie, 1997). The particle displacement is not confined entirely to the surface of the medium. Particles below the free surface are also affected by the passage of the Rayleigh wave. The penetration depth of the surface wave is typically taken to be the depth

at which the amplitude is attenuated to (e^{-1}) of its values at the surface. For Rayleigh waves with wavelength λ the characteristic penetration depth is about 0.4λ.

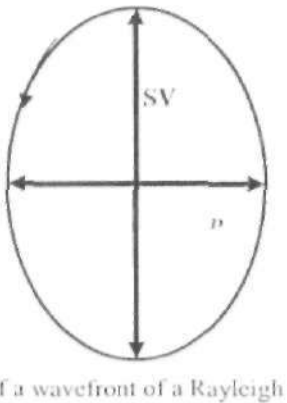


Figure 2.1: The particle motion of a wavefront of a Rayleigh wave consists of a Combination of P and SV vibration in the vertical plane.

(ii) **Love (L) Waves:-** they are surface waves that cause horizontal shearing of the ground. Named after A.E.H. Love, a British mathematician who created a mathematical model of the waves in 1911. They usually travel slightly faster than Rayleigh waves. Depth of penetration of the Love waves is also dependent on frequency, with lower frequencies penetrating to greater depth. They transverse perpendicular to the direction of wave propagation and generally parallel to the Earth's surface. The velocity of Love wave (V_L) is about 2.0 km/s to 4.4 km/s in the Earth which depends on the frequency of the propagating wave and the depth of penetration of the waves. In general, the Love waves travel slightly faster than the Rayleigh waves. Love waves exist because of the Earth's surface. They are largest at the surface and decrease in amplitude with depth. Love waves are dispersive, that is, the wave velocity is dependent on frequency, generally with low frequencies propagating at higher velocity (Lowrie, 1997).

2.2. Reflection and Refraction Surveying

In seismic surveying, seismic waves are created by a controlled source and propagated through the subsurface of the Earth. Some of these waves return to the surface after refraction or reflection at geological boundaries within the subsurface. A direct wave travels along a straight line through the first layer from source to detector with the velocity of the first medium (layer). A reflected ray is obliquely incidented at the interface and is reflected back through the first layer to the detector, with the velocity of the first layer. A refracted ray travels obliquely down to the interface at the velocity of the first layer, then along the interface at the velocity of the second layer and then back to the first layer at the velocity of the first layer. The relative proportions of energy transmitted and reflected are determined by the contrast in acoustic impedance Z across the interface. Acoustic impedance of a rock is the product of its density ρ and its compressional wave velocity v, (i.e. $Z = \rho v$).

The travel-time curves, or time-distance curves for the direct, reflected and refracted rays are shown in figure 2.2 below. A suitable analysis of the travel-time curves for the reflected and refracted ray will aid in the estimation of the depths to the various underlying layers, the location and mapping of the subsurface interfaces. This had led to the two independent seismic surveying methods, namely, REFLECTION SURVEYING and REFRACTION SURVEYING methods, each with its distinctive methodologies and field of application. This curve appears more complex for multiple layer models.

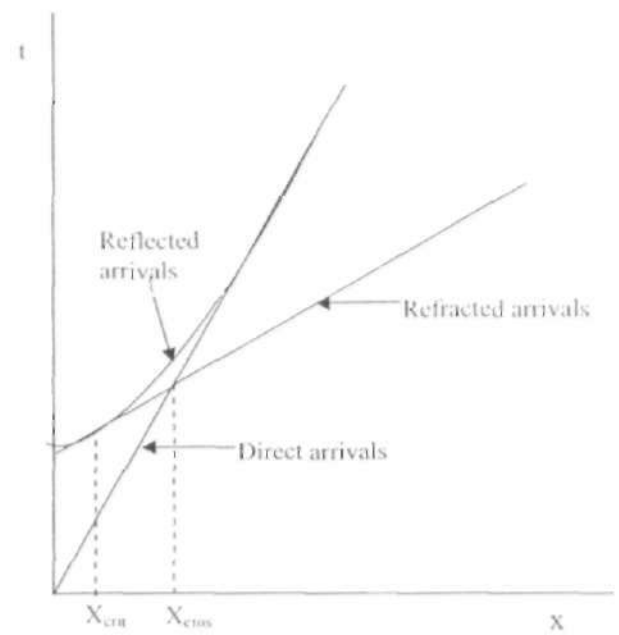


Figure 2.2: Travel-time curve for direct, reflected and refracted rays in the case of a simple two-layer model.

The first arrival of seismic energy at a surface detector offset from a surface source is always a direct ray or a refracted ray. The refracted ray at the crossover distance x_{cross} overtakes the direct ray. Beyond this offset distance the first arrival is always a refracted ray. Since critically refracted rays travel down to the interface at the critical angle there is a certain distance, known as the critical distance x_{crit}, within which refracted energy will not be returned to surface. At the critical distance, the travel times of reflected rays and refracted rays coincide because they follow effectively the same path. Reflected rays are never first arrivals: they are always preceded by direct rays and, beyond the critical distance, by refracted rays also.

The methodology of refraction and reflection surveying is determined by the above characteristics of the travel-time curves. In refraction surveying, recording ranges are chosen to be sufficiently large to ensure that the crossover distance is well exceeded in

order that refracted rays may be detected as first arrivals of seismic energy. Indeed, some type of refraction survey considers only these first arrivals, which can be detected with unsophisticated field recording systems. In general this approach means that the deeper the refractor, the greater is the range over which recordings of refracted arrivals need to be taken.

On the other hand, in reflection surveying, reflected phases are sought that are never first arrivals and are normally of very low amplitude because geological reflectors tend to have small reflection coefficients. Accordingly, reflections are normally concealed in seismic records by higher amplitude events such as direct or refracted body waves and surface waves. Reflection surveying method therefore has been capable of distinguishing between reflected energy and other types of synchronous noise. Recordings are normally restricted to small offset distances, well within the critical distance for the reflecting interfaces of main interest. Since reflections may always be detected at small offset distances there is, in general, no necessity to increase the overall recording range to investigate deeper reflectors (Kearey et al., 2002).

2.3. Seismic Reflection Method

Reflection Seismology - In reflection methods, analysis is concentrated on energy arriving after the initial ground motion. Specifically, the analysis concentrates on ground movement that has been reflected from subsurface interfaces. In addition to examining the times of arrival of these, reflection seismic processing extracts information about the subsurface from the amplitude and shape of the ground motion. Subsurface structures can be complex in shape but like the refraction methods, are interpreted in terms of boundaries separating materials with differing elastic parameters.

Reflection method is directed primarily at finding the depths to reflecting surfaces and the seismic velocities of subsurface rock layers. A seismic signal (example an explosion) is produced at a known place at a known time, and the echoes reflected from the boundaries between rock layers with different seismic velocities and densities are recorded and analyzed.

Geophones are spread out in the region of subcritical reflection, within the critical distance from the shot-point, where no refracted arrivals are possible. Within this distance the only signals received are the waves that travel directly from the shot point to the geophones and the waves reflected at subsurface interfaces. Surface waves are also recorded and constitute an important disturbing noise, because they interfere with the reflected signal. Reflection seismic data are most usually acquired along profiles that cross geological structure as nearly as possible normal to the strike of the structure. The travel-times recorded at the geophones along a profile are plotted as a two dimensional cross-section of the structure. Recently the three-dimensional surveying has mostly been employed.

Several field procedures are in common use. They are distinguished by different layouts of the geophones relative to the shot point. The most routine application of reflection seismology is in continuous profiling, in which the geophones are laid out at discrete distances along a profile through the shot point. After each shot the geophone layout and shot point are moved to a predetermined distance along the profile, and the procedure is repeated. Broadly speaking, there are two main variations of this method, depending on whether each reflection point on the reflector is sampled only once (conventional coverage) or more than once (redundant coverage).

The most common form of profiling method in reflection is the split-spread method (Figure 2.3), in which geophones are spread symmetrically on either side of the shot-point. If the reflector is flat lying, the point of reflection of a ray recorded at any geophone is below the point midway between the shot-point and the geophone (Lowrie, 1997).

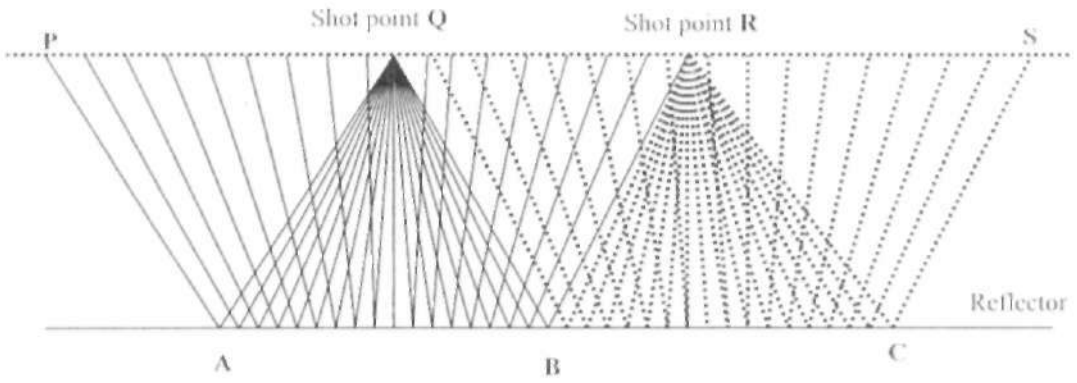


Figure 2.3: The split-spread method of obtaining continuous subsurface coverage of Seismic reflector

2.3.1 Geometry of Reflection Wave Path

In seismic reflection method, since analysis is concentrated on ground movement that has been reflected from subsurface interfaces, the travel time can be inverted to estimate the depth to these interfaces. It is of importance that seismic reflection survey should be carried out in areas where velocity varies with depth, although lateral variation is ignored as a first approximation, (Kearey et al., 2002).

For a single horizontal reflector lying at depth z beneath a homogeneous top layer of velocity v_1, the geometry of the reflected ray path is shown in the figure 2.4 below, a simple case for a single horizontal reflector.

Figure 2.4: The geometry of reflected ray path and time-distance curve for reflected rays from a horizontal reflector.

The equations, that describe the travel time t of the reflected ray from the shot-detector separation x are derived as follows;

$$t = \frac{\sqrt{x^2 + 4z^2}}{v} \tag{2.4}$$

Rearranging equation (2.7) in a normal hyperbolic form gives

$$\frac{v^2t^2}{4z^2} - \frac{x^2}{4z^2} = 1 \tag{2.5}$$

This implies that the travel time-offset distance (time-distance) is a Hyperbola whose axis of symmetry is on the time axis (see figure 2.4).

If x = 0, equation (2.4) becomes $t_0 = \frac{2z}{v}$ which is the intercept on the time axis of the time-distance curve shown above (Kearey et al., 2002)

Equation (2.4) can also be written as:

$$t^2 = \frac{4z^2}{v^2} + \frac{x^2}{v^2} \tag{2.6}$$

thus $$t^2 = t_0^2 + \frac{x^2}{v^2} \tag{2.7}$$

From equation (2.6), $$t = \frac{2z}{v}\left[1+\left(\frac{x}{2z}\right)^2\right]^{\frac{1}{2}} \tag{2.8}$$

$$t = t_0\left[1+\left(\frac{x}{vt_0}\right)^2\right]^{\frac{1}{2}} \tag{2.9}$$

Using the binomial expansion, and for small offset-to-depth ratios, that is, $\frac{x}{vt_0} << 1$. Equation (2.9) can be truncated to obtain.

$$t = t_0\left[1+\frac{1}{2}\left(\frac{x}{vt_0}\right)^2\right] \tag{2.10}$$

Equation (2.10) forms the most convenient form of the time-distance equation for reflected ray. The difference in the travel times ($t_2 - t_1$) for reflected ray arrivals at two offset distances x_1, x_2 is called **moveout**, which is expressed as;

$$t_2 - t_1 = \frac{x_2^2 - x_1^2}{2v^2 t_0} \tag{2.11}$$

A **normal moveout** (NMO) is the difference in travel times ΔT between reflected ray at distance x and zero offset and is given by;

$$\Delta T = t_x - t_0 = \frac{x^2}{2v^2 t_0} \tag{2.12}$$

Where t_x is the time at distance x

This implies that; $$v = \frac{x}{(2t_0 \Delta T)^{\frac{1}{2}}} \tag{2.13}$$

2.3.2 Dipping horizontal reflectors.

If a dip angle is included into the time distance equation (equation 2.4) as an unknown, the expression above becomes;

$$t = \frac{(x^2 + 4z^2 + 4xz\sin\theta)^{\frac{1}{2}}}{v} \tag{2.14}$$

and in hyperbolic form;

$$\frac{v^2 t^2}{4z^2 \cos^2\theta} - \frac{(x + 2z\sin\theta)^2}{(4z^2\cos^2\theta)} = 1 \tag{2.15}$$

The axis of symmetry of the hyperbola is now no longer the time axis. Expanding equation (2.15) binomially, it can be truncated to obtain;

$$t = t_0\left[1 + \frac{x^2 + 4xz\sin\theta}{2v^2 t_0^{\,2}}\right] \tag{2.16}$$

Consider figure 2.5 below, the reflected ray path for an equal offset x updip and downdip from a central shot point, is different in length, hence the two have different travel times. Dip moveout ΔT_d is therefore defined as the difference in travel times t_x and t_{-x} for the reflected ray from the dipping interface to receivers at equal and opposite offsets of x and -x. Therefore, $$\Delta T_d = t_x - t_{-x} \tag{2.17}$$

By using the definition of equation (2.16),

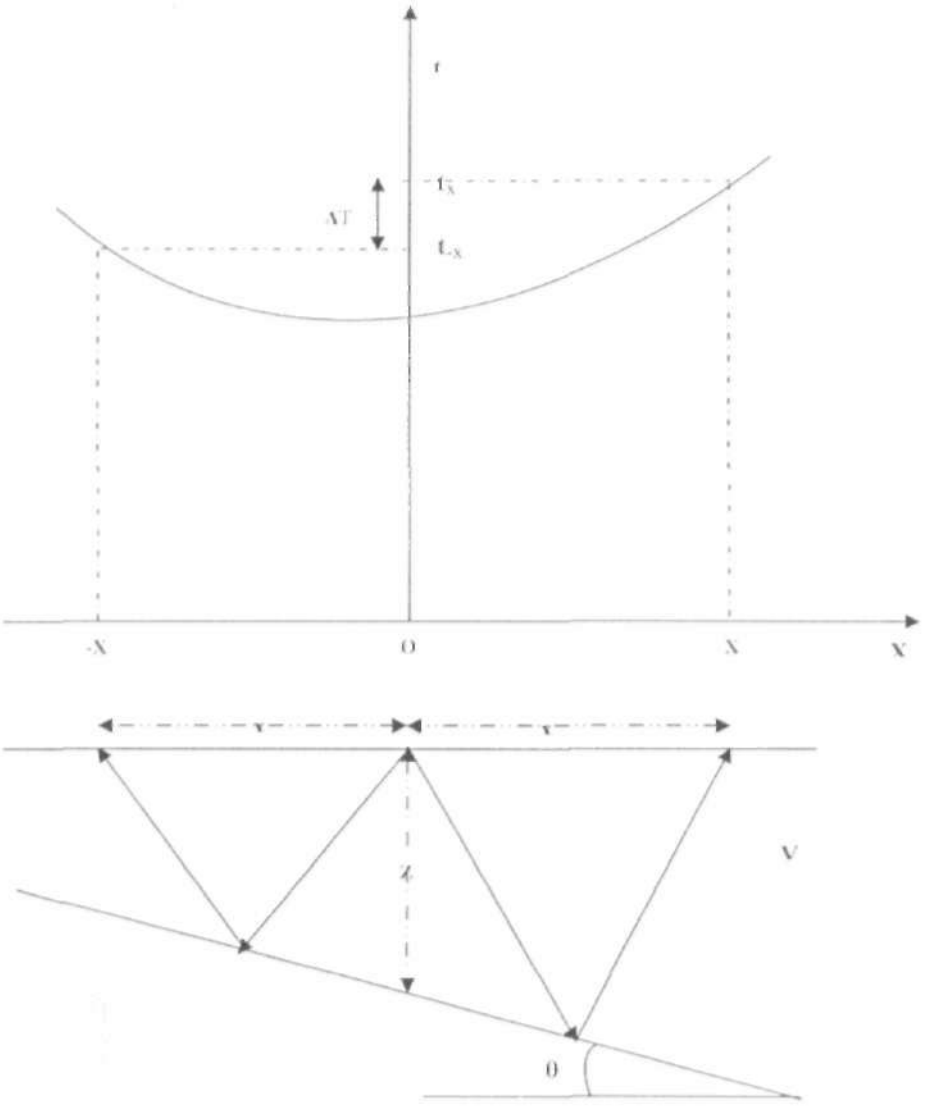


Figure 2.5: The geometry of reflected ray path and time-distance curve for reflected rays from a dipping reflector.

$$\Delta T_d = \frac{2x\sin\theta}{v} \tag{2.18}$$

For small angel of dip, $\sin\theta \approx \theta$

$$\text{Therefore, } \theta \approx \frac{v\Delta T_d}{2x} \tag{2.19}$$

Hence, if v is known, the dip moveout ΔT_d may be used to compute the reflector dip θ.

2.3.3. Ray paths of multiple reflections

So far single ray paths have been considered (known as primary reflector); however there are many paths in a layered subsurface by which a ray can return to the surface after reflection at more than one interface. Such rays are called reverberations, multiple reflections or simply multiples.

Multiples generally have lower amplitudes (than primary reflection) due to loss of energy at reflector. They occur generally at interfaces where there are variations in the reflection coefficient. Ghost reflection occurs when rays are reflected back at the base of a weathered layer, from buried explosive. Water layer multiples occur when a source ray is repeatedly reflected at the seabed and sea surface.

It is important to identify multiple reflections before interpretation because they some time arrive shortly after the primary rays to mask the result. This can cause error in results (Kearey et al., 2002).

2.4. Seismic Refraction Method

The geophysical property that is measured in seismic refraction is seismic velocity. In seismic refraction surveys, the most important kinds of waves are the P-wave (a compressional, longitudinal wave). P-waves propagate at the highest velocity of any seismic waves and are therefore commonly used to pick the first breaks of seismic waves that propagated through earth materials.

These waves move through the subsurface layers. The density of a layer and its elastic properties determine the speed or velocity at which the seismic wave will travel through the layer. The porosity, mineral composition, and water content of the layer affect both its

density and elasticity. A list of the range in compressional wave velocities in common geologic materials are shown in Table 2.1 below. It can be seen from these values that the seismic velocities for different types of soil and rock overlap, and so knowing the velocities of these layers alone does not permit a unique identification of their composition.

Table 2.1: Compressional wave velocities in Earth materials

Rock Type	P-wave velocity (m/s)
Sand (dry)	200 – 1000
Sand (saturated)	1500 – 2000
Clay	1000 – 2500
Sandstone	2000 – 6000
Granite	5500 – 6000
water	1400 – 1500

However, if this knowledge is combined with geologic information, it can be used intelligently to identify geologic strata. In general, velocity values are greater for:

- dense rocks than light rocks.
- older rocks than younger rocks.
- igneous rocks than sedimentary rocks.
- solid rocks than rocks with cracks or fractures.
- unweathered rocks than weathered rocks.
- consolidated sediments than unconsolidated sediments.
- water-saturated unconsolidated sediments than dry unconsolidated sediments.
- wet soils than dry soils.

Figure 2.6 shows a schematic view of a 24-channel seismic system in use and the compressional wave paths through a two-layered system of soil over bedrock. A seismic

source produces seismic waves which travels in all directions into the ground. However, the seismic refraction method is concerned only with some of the waves. One of these waves, (the direct wave) travels parallel to the surface of the ground. A seismic sensor (geophone) detects the direct wave as it moves along the surface layer. The time of travel along this path is related to the distance between the sensor and the source and the material composing the layer (Zhao and Kayal, 2000).

If a denser layer with a higher velocity, such as bedrock, exists below the surface soils, some of the seismic waves will be bent or refracted as they enter the bedrock. This phenomenon is similar to the refraction of light rays when light passes from air into water and is described by Snell's law. One of these refracted waves, crossing the interface at a critical angle, will move parallel to the top of the bedrock at the higher velocity of the bedrock. The seismic wave travelling along this interface will continually release energy back into the upper layer by refraction. These waves may then be detected in the surface at various distances from the source (Figure 2.6). Beyond a certain distance (called the critical distance), the refracted wave will arrive at a geophone before the direct wave. This happens even though the refraction path is longer, because a sufficient portion of the wave's path occurs in the higher velocity bedrock. Measurement of these first arrival times and their distances from the source permits calculation of layer velocities, thicknesses and bedrock depth. Application of the seismic method is generally limited to resolving three to four layers. The preceding concepts are based upon the fundamental assumptions that:

1. Seismic velocities of geologic layers must increase with depth. This requirement is generally met at most sites.
2. Layers must be of sufficient thickness to permit detection.
3. Seismic velocities of layers must be sufficiently different to permit resolution of individual layers.

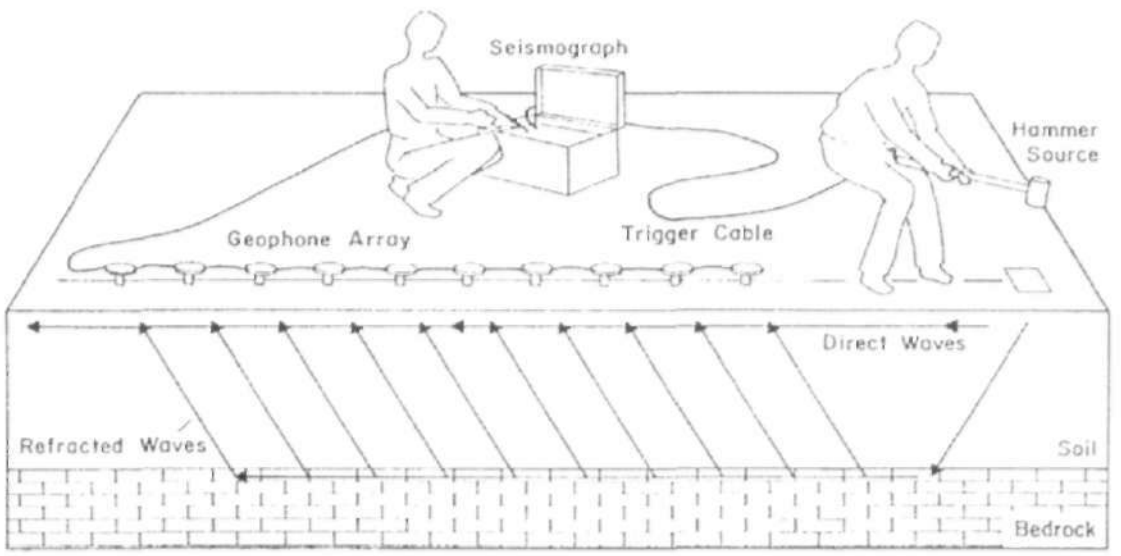


Figure 2.6: Field layout of a seismograph showing path way of direct and refracted waves for a two-layer soil/ rock system.

Data are recorded on a seismograph and later downloaded to a computer for analysis of the first-arrival times to the geophones from each shot position. The seismograph is an instrument which electronically amplifies and then displays the received seismic signal from the geophone. The identification and measurement of the arrival time of the first wave from the seismic source is obtained from its displayed presentation. The time is measured in milliseconds, with zero time or start of trace initiated by the source, which provides a trigger signal to the seismograph. The arrival time is plotted against source-to-

geophone distance producing a time/distance (T/D) plot as shown in figure 2.7 below. From a time/distance plot, it is important to know that;

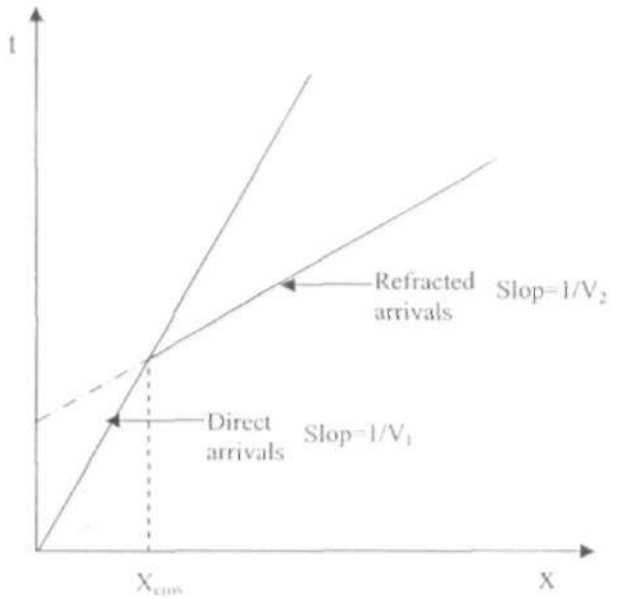


Figure 2.7: Travel-time curve for the direct and the refracted waves from a single horizontal refractor

(i) The number of line segments indicates the number of layers.

(ii) The slope of each line segment is inversely proportional to the seismic velocity in the corresponding layer.

(iii) Break points in the plot (critical distance, X) are used with the velocities to calculate layer depth.

The primary applications of seismic refraction are for determining depth to bedrock and bedrock structure, for mapping thickness of weathered layer, for determining depth to water table, for engineering purpose as well as applying correction to reflection data. The technique has been successfully applied to mapping depth to basement of backfilled quarries, depth of landfills, thickness of overburden and the topology of the bed rock. Refraction surveys yield data on seismic velocities of the various formations as well as on

their geometry and often make it possible to identify formations, which are mapped. However reflection method is used for deeper probing. The refraction method is particularly valuable for reconnaissance in areas were structures have a large relief and where there is at least one high speed marker bed overlain by lower speed formations.

2.4.1 Geometry of Refracted Ray Path; Planar Interfaces

Some general assumptions considered for the ray geometry are that: the velocity within each layer is uniform, the velocity increases with depth, the subsurface is composed of a series of layers separated by plane (possibly dipping) interfaces and ray paths are restricted to a vertical plane containing the profile, i.e., no component of the cross dip.

2.4.2 Two-layer case with horizontal interface

Consider figure 2.8 below showing the path of a ray as it travels from the shot point A through the Earth B, C and then to the detector D on the earth surface.

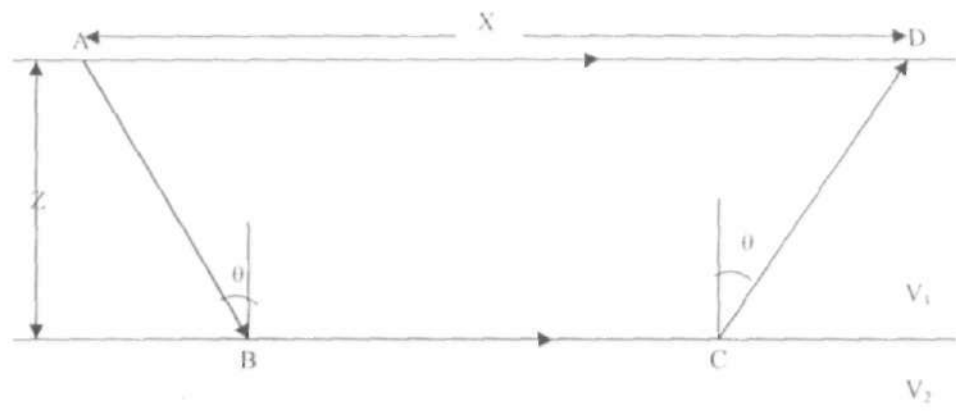


Figure 2.8: The direct and the refracted waves through a two-layer model. Individual ray path from source A to detector D as shown.

The direct ray travels horizontally through the top of the upper layer from A to D at velocity V_1. The refracted ray travels down to the interface B at velocity V_1 and along the

interface between B and C at velocity V_2. And then back to the top D at a distance of X from the shot point A.

The total travel time therefore along the refracted ray path ABCD is;

$$t = t_{AB} + t_{BC} + t_{CD} \tag{2.20}$$

$$t_{AB} = \frac{z}{v_1 \cos\theta} \tag{2.21}$$

$$t_{CD} = \frac{z}{v_1 \cos\theta} \tag{2.22}$$

$$t_{BC} = \frac{x}{v_2} - \frac{2z\tan\theta}{v_2} \tag{2.23}$$

$$t = \frac{x - 2z\tan\theta}{v_2} + \frac{2z}{v_1 \cos\theta} \tag{2.24}$$

where $\sin\theta = \frac{v_1}{v_2}$ (Snell's Law) and $\cos\theta = \left[1 - \frac{v_1^2}{v_2^2}\right]^{\frac{1}{2}}$

Equation (2.24) can be expressed as

$$t = \frac{x\sin\theta}{v_1} + \frac{2z\cos\theta}{v_1}$$

$$t = \frac{x}{v_2} + \frac{2z\sqrt{v_2^2 - v_1^2}}{v_2 v_1} \tag{2.25}$$

$$t = \frac{x}{v_2} + t_i \tag{2.26}$$

$$t_i = \frac{2z\sqrt{v_2^2 - v_1^2}}{v_2 v_1} \tag{2.27}$$

where t_i is the intercept on the time axis of the travel time curve, whose gradient is $\frac{1}{v_2}$

Solving for refractor depth,

$$z = \frac{v_2 v_1 t_i}{2\sqrt{v_2^2 - v_1^2}} \tag{2.28}$$

Note, that at the crossover distance X_{cros}, the travel time of the direct rays and the refracted rays are equal.

$$\frac{X_{cros}}{v_1} = \frac{X_{cros}}{v_2} + 2z\frac{\sqrt{v_2^2 - v_1^2}}{v_2 v_1} \tag{2.29}$$

Thus $$x_{cros} = 2z\sqrt{\frac{v_2 + v_1}{v_2 - v_1}} \tag{2.30}$$

Equation (2.30) shows that the crossover distance is always greater than twice the depth to the refractor.

2.4.3. Three layer case with horizontal interfaces

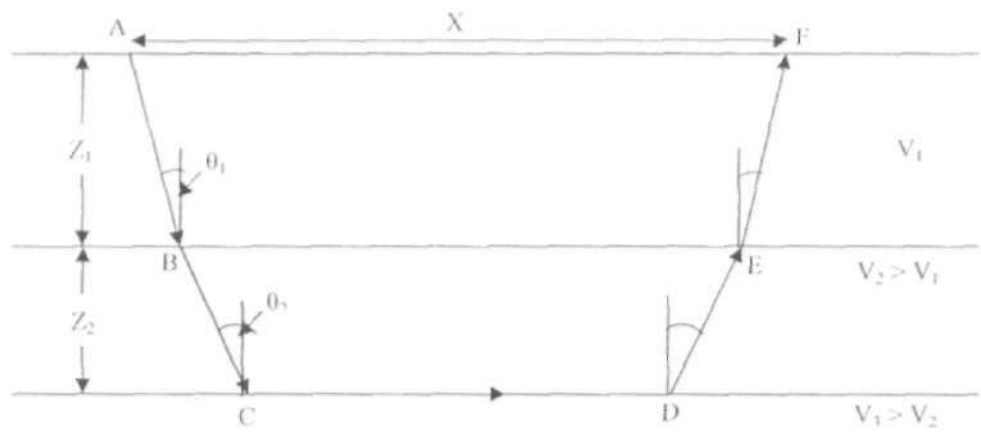


Figure 2.9: The refracted ray path through the bottom layer of a three-layer model

By analogy with the previous equation (2.20), the travel-time along the refracted ray path ABCDEF (as shown in figure 2.9 above) to an offset distance x is given by;

RASHID IBR KIM LIBRARY

$$t = \frac{x\sin\theta_1}{v_1} + \frac{2z_1\cos\theta_1}{v_1} + \frac{2z_2\cos\theta_2}{v_2} \tag{2.31}$$

Where $\theta_1 = \sin^{-1}(\frac{v_1}{v_2})$, $\theta_2 = \sin^{-1}(\frac{v_2}{v_3})$

This implies that $$t = \frac{x\sin\theta_1}{v_1} + t_{i1} + t_{i2} \tag{2.32}$$

where t_{i1} and t_{i2} are the intercepts on the time axis of the travel time curve for rays critically refracted at the upper interface and lower interface respectively (Kearey et al., 2002).

2.4.4. Dipping-layer case with planar interfaces

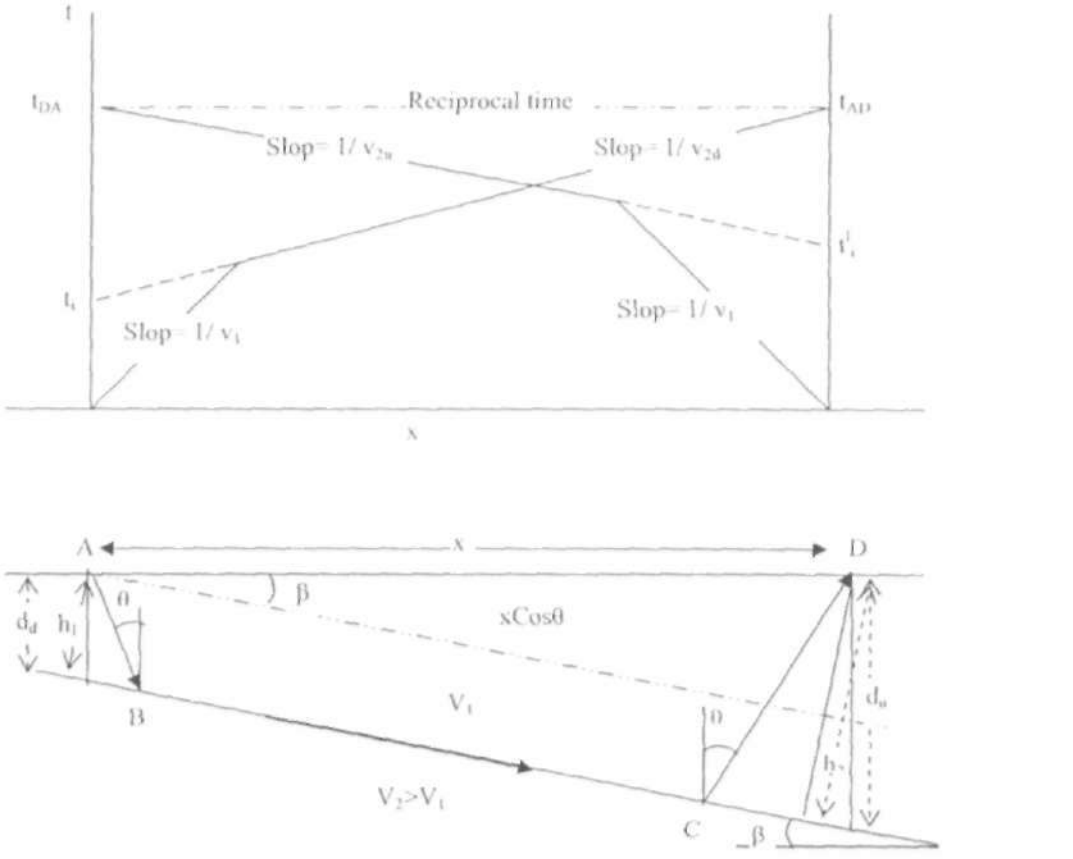


Figure 2.10: Travel-time curves for a refracted ray arriving from a dipping refractor in the forward and reverse direction along a refraction profile line

The ray ABCD (figure 2.10 above) from the shot-point A strikes the interface at the critical angle 0 at B, runs as a head wave with velocity v_2 along the dipping interface and the ray emerging at C eventually reaches a geophone at the end of the profile at D. During reverse shooting, the ray from the shot-point at D to a geophone at A transverses the same path in the reverse direction. However the t-x curves are different for the up dip and down dip shots. Let d_d and d_u be the perpendicular distances from the points D and A to the interface CB respectively. For the down-dip shot at A the travel time to distance x is given by:

$$t_{AB} = \frac{(AB+CD)}{v_1} + \frac{BC}{v_2} \text{ (Dobrin, 1976)} \tag{2.33}$$

$$t_d = \frac{x}{v_1}\sin(\theta+\beta) + t_i \tag{2.34}$$

where t_i is the intercept time for the down dip shot:

$$t_i = \frac{2h}{v_1}\cos\theta \tag{2.35}$$

In the same process analysis for shooting at the up dip is analogous and is given as;

$$t_u = \frac{x}{v_1}\sin(\theta-\beta) + t_i' \tag{2.36}$$

where t_i' is the intercept time for the up-dip shot:

$$t_i' = \frac{2h_2}{v_1}\cos\theta \tag{2.37}$$

KASHIM IBRAHIM LIBRARY

The perpendicular distance h_2 to the interface comes from the intercept time t_i^1 as stated above. Therefore;

$$h_2 = \frac{v_1 t_i^1}{2\cos\theta} \qquad (2.38)$$

A similar expression is obtained for h_1 in terms of t_i .The depth d_u at the up dip and down dip d_d are;

$d_u = \frac{h_2}{\cos\theta}$ and $d_d = \frac{h_1}{\cos\theta}$ respectively.

2.5. Elevation and Weathering Corrections for Refraction and Reflection Data

Refraction times must be corrected for elevation and changes in the thickness of the weathered layer. The former correction removes differences in travel times due only to variations in the surface elevation of the shots and detector stations. The weathering correction removes differences in travel times through the near surface zone of unconsolidated, low speed sediments, which may vary in thickness from place to place.

It is necessary to correct the data on reflection records for differences in surface elevation and for the travel time in the weathered layer. The corrections are similar in principle to those employed in refraction work, but there are some differences in their mode of computation (Dobrin, 1976).

2.6 Refraction Tomography

Tomography is an imaging technique that generates a cross-sectional picture of an object by utilizing the object's response to the nondestructive, probing energy of an external

RECEIVED

source. Seismic Tomography makes use of sources that generate seismic waves to probe a geological target of interest (Tien-when and Philip, 1994).

Several tomographic techniques have been applied to seismic first arrival travel time data profile. Tomographic techniques develop best-fit velocity models by iteratively comparing different velocity structures with observed data to a degree of resolution specified by the modeler. Greater resolution, however, does not imply improved accuracy. The tomographic analyses presented in this thesis used a simulated annealing procedure, where a controlled Monte-Carlo inversion is used to develop a globally optimized velocity model of the subsurface. The method uses only first arrival time data and profile geometry as input. No initial assumptions of velocity structure or layering are required. As such, the method is easily applied and is well suited for investigation of areas dominated by complex shallow structure, significant velocity gradients and variable topography. Another advantage of Tomography is that the minimum curve ray-path in the inversion defines a maximum depth of investigation whereas only estimates of the investigation depth are possible using more traditional methods. In cases where insufficient data exist, any tomographic inversion may generate false models. Therefore, in acquiring Tomography data shots have to be taken at each geophone point. The first shot taken at the beginning of the profile, will give only a forward travel time and no reverse, the next shot taken at the first geophone will give a forward travel time, but zero reverse travel time. The shot taken at the second geophone will produce a forward travel time and a small reverse travel time. The shot taken at the centre of the spread will produce equal forward and reversed travel time. The shot taken at the end of the profile will produce only reverse travel time with zero forward travel time as shown in Figure 2.11. Multiple shot points along a survey

profile provides greater data coverage for analysis and aids in generating a more accurate model.

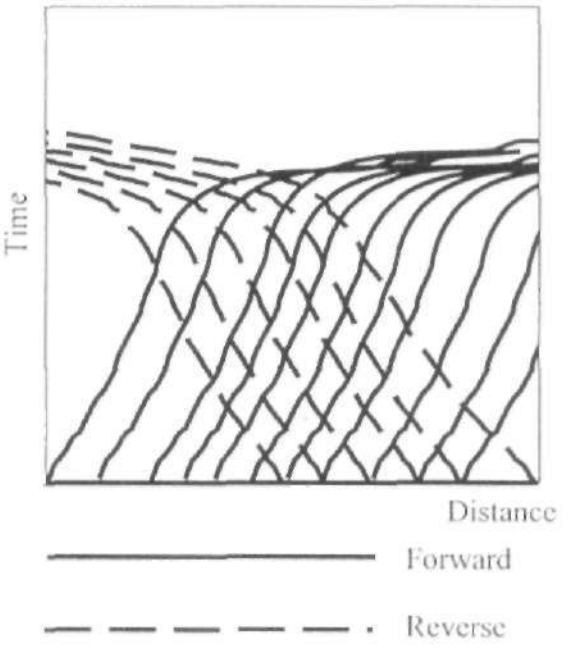


Figure 2.11: Forward and reverse travel time curve for Tomography data

CHAPTER THREE

INSTRUMENTATION AND FIELD PROCEDURE

3.1 Instrumentation

The basic 24-channel Terraloc Mk6 is a self-contained multi-channel seismograph for cost-effective refraction and high-resolution reflection surveys, tomography, and more. This instrument has been designed to function in all kinds of weather condition, hence, its suitability worldwide. Some of its extraordinary and powerful features include the following:

(i) Excellent resolution that makes use of 18 bit ADC (analog/digital converter) and 3 bit IFP (instantaneous floating point) amplifier.

(ii) Fully compatible with office computer, using Microsoft MS-DOS version 6.0, an internal 80-280 MB hard disk, 3½ inch disk drive, and use of SEG2 standard data file format.

(iii) Usable with various energy sources (even the new mini-vibrators) with record length settings from 128 to 16384 samples in eight steps.

(iv) Field quality control measurements is possible using geophone test, noise monitoring, and a wide choice of single or multi-trace view modes.

(v) Full control and selection of all operating functions can be done from two top panel keyboards with 28 keys. When in the office, a PC-AT keyboard and serial mouse can be connected for convenience.

(vi) Excellent results for tomography and high-resolution seismic, can be obtained by varying sampling rates from 25 μs to 2 ms in steps.

(vii) Possibility of displaying full screen of records of traces, automatic pick of first arrivals, list of first arrival times, velocity calculation, frequency analysis of single traces.

(viii) Low weight, only 16kg, small volume, only $0.03m^3$, all in a robust water casing.

Terraloc Mk6 has output port for a printer, a serial mouse, an external keyboard and monitor. Terraloc Mk6 offers a wide range of sampling interval (25μs to 2ms) and number of records to choose. The desired values can be set up from the 'measure menu' Figure 3.1. It is important to note that long sampling interval gives low number of samples and contains less information, hence difficulty in interpretation, while short sampling interval gives high number of samples with good information for interpretation, but it occupies a larger storage space.

Also included in the measure menu is the layout geometry screen, which allows the entry of the exact layout geometry in three dimensions generally along, across, and up or down the profile. The coordinate system comprises X, Y and Z fields. Normally X is distance along, Y is distance perpendicular to the layout and Z is height above or below the layout. The layout geometry screen also contains the source type and receiver type option settings.

Figure 3.2 shows the 'view data' menu screen comprising three sections; the information window, the command window and the data window. The information window is located at the top, and as its name implies, contains information (like sample intervals, trace, time etc.) about the current record, which is displayed, on the screen. There are three modes of display: all traces, single trace (or zoom), and spectrum form. The command window (located to the right of the page) consists comprised of ten command buttons; each (except

the last one) is preceded by a quick access number. The data window is the largest part, located towards the left, it displays the graphical trace.

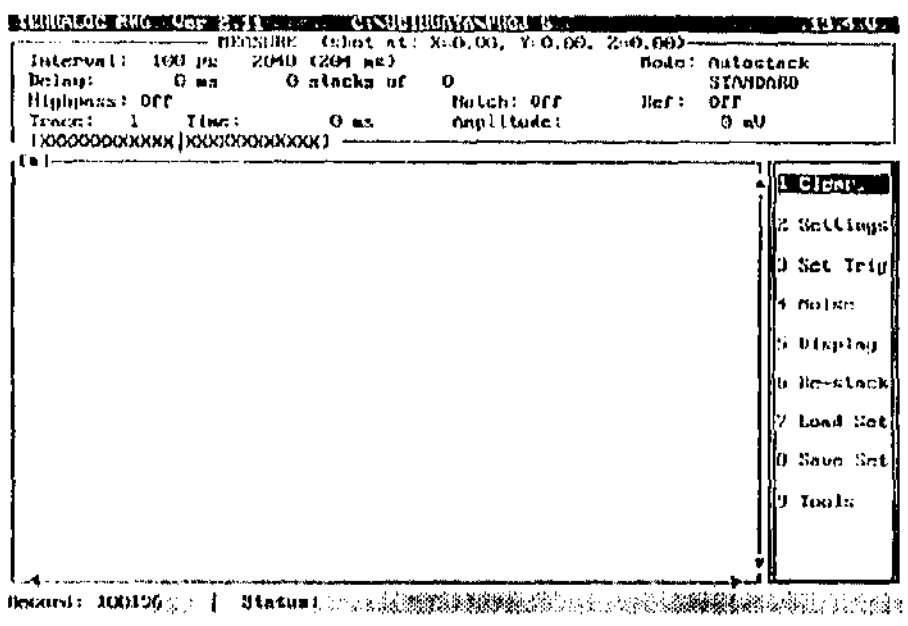


Figure 3.1: Measure Menu

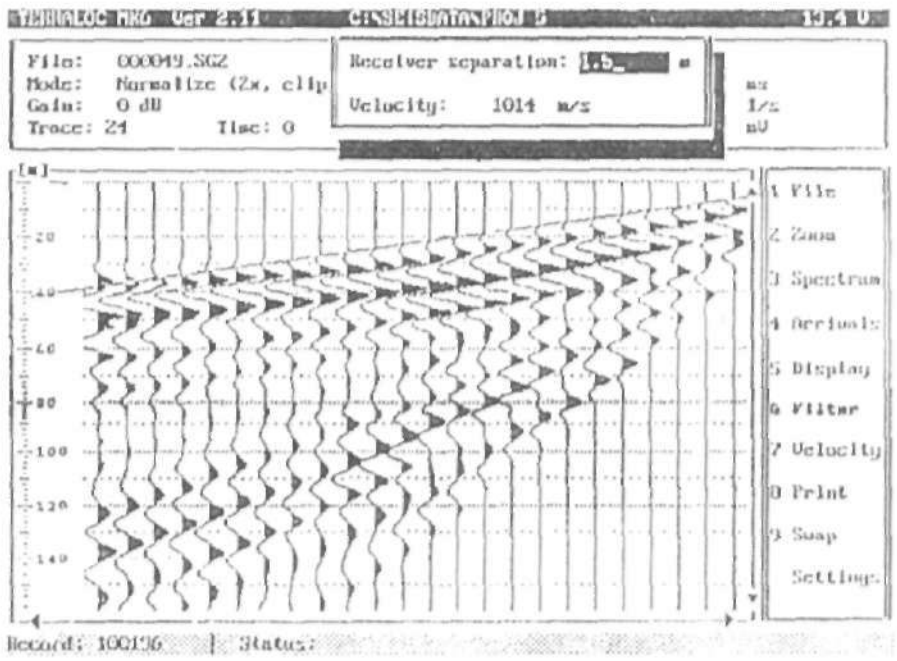


Figure 3.2: The view data menu

Velocity calculation can be done by moving the velocity line (Figure 3.2) across the screen. When the line is tilted, the window on top displays a velocity corresponding to the tilts figure. In this way, the velocity line can be moved and tilted in such a manner that it correlates with e.g. first arrivals in a refraction record. Thus the velocities for different layers can easily be determined.

First arrival times can be picked either automatically or manually from the data. Already existing first arrivals, can easily be edited, saved to disk, read from disk and cleared from memory.

Spectrum analysis can also be carried out using Terraloc Mk6. The spectrum can be used to estimate cutoff frequencies for the digital filters. It can also be used to analyze ground noise for optional setting of the analog high pass and notch filters.

The Terraloc Mk6 software is not meant to be used as a replacement for dedicated seismic processing, interpretation and modelling software. However, there is always a need to be able to do some digital filtering, which is also possible with the Terraloc MK6.

The Terraloc Mk6 has a software disk and a disk width sample records. Each disk installs the content automatically. Also to be used with Terraloc Mk6 are sets of 25, 45 Hz to 100 Hz vertical geophones. Twenty-four (24) geophones are connected to the twenty-four takeouts on the cable feeding the twenty-four channels, with the remaining one acting as trigger geophone.

3.2 Preliminary Preparations

Although, resistivity survey has been done around this area (main campus) there is also the need to carry out seismic survey to justify some long time effects on erected structures. The geology of the area has been well established from studies carried out around the Kubanni river region, this can be interpolated up to the main campus area. The sinking and cracking of student hostels has initiated the urge to carry out a detailed study over some prone areas to investigate the subsurface structure of some student hostels.

Based on the above considerations the period for the fieldwork was fixed for about three weeks. Prior to this period, negotiations and application permissions had to be granted to enter any of the student hostels. Therefore the month of June was for the preparation of the fieldwork. Preliminary testing of the equipment (Terraloc Mk6) was carried out on regular basis in front of the Physics Department. Having tested the equipment successfully the final date for the fieldwork was fixed. The map of the study area was collected, and the site

for each of the borehole to be correlated, was located. Their positions were noted, which was used as a guide in planning the layout geometry of the profiles.

3.3 Testing of the Equipment

With the sophistications of the seismic equipment now, the whole equipment has been compacted together in bulk, like a mobile portable computer system. The most important instrument is the Terraloc Mk6 and the vertical geophones (Figure 3.1). The best results from any experimental work will depend on the functionality of the equipment and weather constrain (rain, wind), among others. To attain the best precisions from the results, the Terraloc Mk6 was tested for three weeks to ascertain its effectiveness and sensitivity.

The instrument was tested by making use of the Terraloc Mk6 keyboard which has 28 keys divided into numerical (upper) and command (lower) keys. External PC-AT keyboard was also used during the process of testing the equipment. Terraloc has a main menu bar, which contains the file menu, measure menu and view menu. The file menu, contains the file manager, which enables the copy, delete, make directory, change directory, remove directory and format commands. Another important menu is the "Measure" menu which contains the sampling parameter that enables the selection of the different sampling intervals and number of samples. Also included in the settings is the layout geometry that gives the opportunity to enter geophone spacing and shot location in three dimensions. The view menu is mainly for viewing the traces. All the traces can be viewed at the same time or single trace (or zoom) and in spectrum form. Filtering, final editing and velocity calculation is carried out under view menu.

Different layout geometries, which include forward profiling, reverse profiling and split spread profile, were explored during the period of testing. Different sampling techniques were used to observe the effectiveness of the traces. The input of the different channels was carefully observed. The importance of the trigger geophone whose function is to trigger the equipment was obvious during the testing of the equipment. The equipment test was carefully and properly carried out, to ease logistic problems in the field and to reduce error in the data collected.

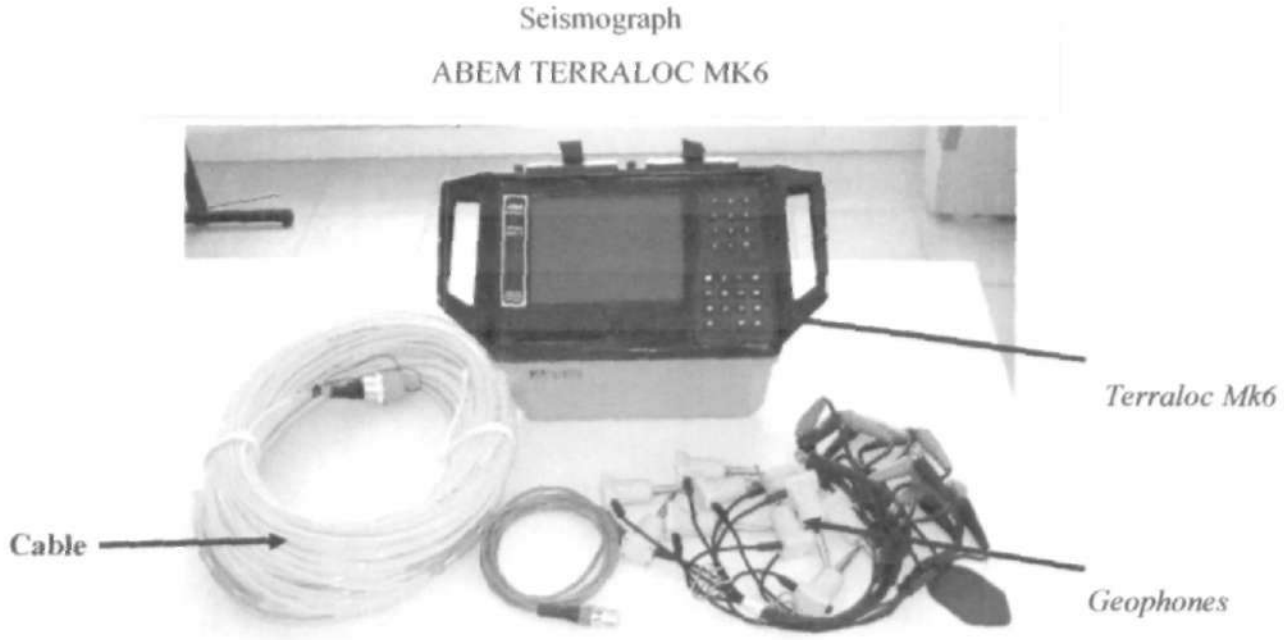


Figure 3.4: Terraloc Mk6, some sets of geophones and reels

3.4 Factors to be considered for Field Use

The seismic line must be centre over the required information area and overall line length must be three to five times the maximum depth of interest. Geophone spacing requires closer spacing of between 3 to 15 meters wide for shallow geophysical study. Repetition of seismic refraction lines along a traverse will reveal lateral variations. Resulting data can be used to indicate trends of dipping layers and to detect anomalous conditions, such as fractures and disturbed zones. Since the presence of a dipping layer may not be known immediately on the field, it is necessary to run both forward and reverse lines to obtain true velocities and depths, if the geologic beds are not horizontal. A reverse line is simply a second set of seismic measurements with the source located at the opposite end of the same line of geophones.

Typically, velocity anomalies (low velocities) will occur as the array crosses a disturbed soil zone such as a trench. Figure 3.4 below show a typical waveform from a single geophone. Multichannel seismographs unlike the single channel, increase the rate of data acquisition using an array of 6, 12, 24 or more geophones. All geophone signals are recorded simultaneously after initiation from a single hammer blow. The display of simultaneous waveforms enables the operator to measure arrival time by noting trends in the composite data set. This is especially useful in noisy areas. More sophisticated instruments commonly incorporate a considerable amount of control over gain and filtering of the signals, which is of great use on difficult or "noisy" sites.

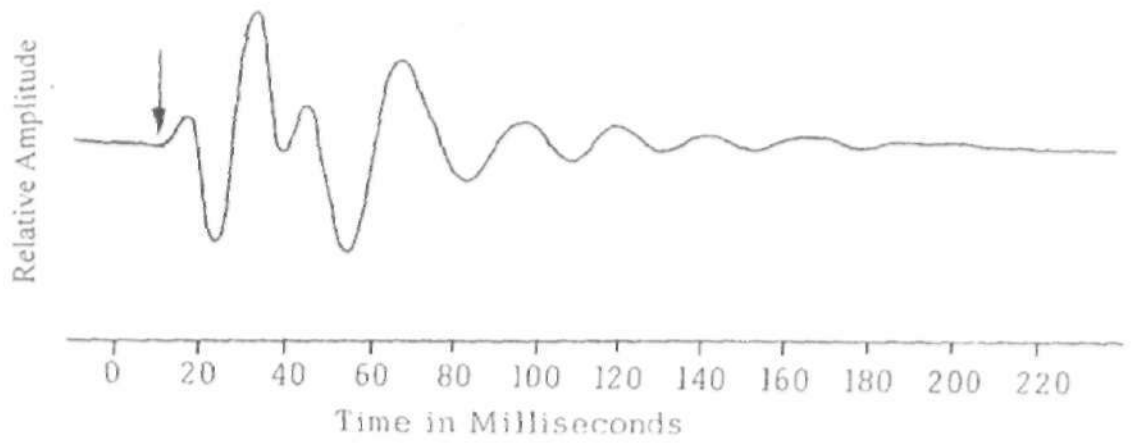


Figure 3.4: Typical seismic waveform from a single geophone. Arrow marks arrival of first compressional wave.

Since the seismic method measures ground vibration, it is inherently sensitive to noise from a variety of sources. Signal enhancement is a significant aid when working in noisy areas and with smaller energy sources. Enhancement capability is available in most single and multi-channel systems. Enhancement is accomplished by adding a number of seismic signals from repeated hammer blows. The coherent seismic signal is increased in direct proportion to the number of blows, while random noise in the seismic signal is increased only by the square root of the number of blows. This causes the seismic signal to "grow" out of the noise level, permitting operation in noisier environments and at greater hammer-to-geophone spacing. The overall results provide a more accurate measurement of the first arrival time. Depending on site conditions, a hammer is useful for obtaining seismic data to depths of 10 to about 40 m; while a 250 kg (500-pound) drop weight is required for depths of 50 to 100 m. A more powerful seismic source is necessary to obtain deeper data or for work in noisy areas although many sources are available for meeting specialized needs.

(i) Quality Control

Quality control can be achieved in several ways:

- A check of the seismic signal and noise conditions on the instrument display verified the proper functioning of geophones and trigger cables and the correct setting of the instrument.
- Background or off-site data is often required for correlation to known geologic information and to establish clean background data. This information is also useful as a reference for evaluating complex site conditions.
- Boring logs should be obtained to minimize the possibility that low velocity (hidden layers) or thin beds will remain undetected.

(ii) Noise

Seismic signals are strongly affected by ground vibration noise; less so by geologic scatter.

In addition, the subjective pick of first arrival time can contribute a few milliseconds of error. Unwanted vibrations which affect the seismic signal at the geophone may be caused by:

- Strong winds which move nearby trees;
- Sounds of airplanes;
- Surface sources, such as moving vehicles on nearby high-ways and railroads;
- Field crews walking near geophones;
- Nearby blasting or operation of heavy construction equipment.

Geologic scatter may be caused by lateral variation in layer composition or an irregular interface between layers. Such scatter can complicate interpretation of the T/D plot, but it is also a valuable indicator of condition of the site. Examples include:

- Variations in the thickness of the "soil zone";
- Boulders in glacial clay or till;
- Zones of increased cementation in sandstone and limestone;

- Lenses of sand in clay layers;
- Variations in saturated water content caused by perched water tables;
- Irregular bedrock surfaces;
- Limestone containing numerous cavities.

3.5 Field Procedure

After assembling the equipment for the survey, a field party was constituted, made up of the author, driver and labourers. The fieldwork commenced on 28th June 2006. A total number of 8 profiles was taken for this investigation. The data was collected for tomography using the forward and reverse profiling method with a sampling interval of 250 μs. A total of 720 sample shot was recorded.

The instrument underwent some memory test before getting to the main menu. A geophone test was carried out at each profile to check the level of noise and for any unconnected geophone. The instrument was then armed under the measure menu, and ready to receive signals. The geophones were laid out at intervals of 5 m (in all profile) along side the reel cable and then connected at the various takeouts on the cable. The position of the first geophone was noted based on the direction of the forward profile and its connection to the instrument. The direction of most of the profiles was mainly East-West, due to the availability of profile-able lengths. With the Terraloc Mk6 placed at the centre of the spread, and all necessary connections of cables, trigger coil and powers made to their appropriate channels, shots were taken on the base plate placed beside each geophone and the trigger geophone. For hard-ground areas, a little hole is bored in the ground before inserting the geophones. Each geophone had a good vertical contact with the ground.

Seismic energy was sent into the ground with the aid of hammer blow; this triggered the instrument, which records the ground vibration. Shot was taken at each geophone and at each end of the profile, with offset for both the forward and the reverse profiles. The data was saved, and the instrument was assembled and taken to the next profile.

3.6 Problems encountered on the field

The problems encountered in the field include:

(i) Hardness of the ground.

(ii) The battery occasionally ran down after being used for a long time, which caused delay and incurred expenses of the fieldwork.

(iii) When taking data readings on a busy road, the noise of cars and passersby constituted a lot of seismic noise, which can mask the real signal.

(iv) Since the area is already built-up, it was difficult to obtain a perfect straight profile line in some of the profiles taken and some offset extendes in to tarred roads or close-by buildings along the profile lines.

3.7 Data Collection

The data collected at each layout include:

(i) Date of the survey

(ii) Type of layout

(iii) The sampling interval

(iv) The number of samples

(v) The record file number

(vi) The height of the layout

All other information was stored in the memory of Terraloc Mk6.

3.7.1 Precautions taken to ensure good result

(a) Observation of traffic and movement within the survey area.

Before any reading was taken, it was ensured that there was no movement of any kind close to the layout, which could constitute noise, by observing the flow of traffic within the survey area.

(b) Placement of geophones

The geophones were always pushed into the ground to make good contact with the ground. And they were placed so that they could maintain a vertical position since they were vertical geophones.

(c) Placement of the trigger geophones

The trigger geophone was placed close to the shot point as much as possible in order to have good onset time in the record.

(d) Problem of offset

In the event of any offset at the shot point or of the geophone position the distance was noted and updated in the record.

CHAPTER FOUR

DATA PROCESSING AND INTERPRETATION

4.1 Introduction

All raw data collected in the fields, are impregnated with all sort of unwanted features and to interpret such a data, rigorous mathematical deduction will be involved, time and money will also be incurred only to obtain a result which will not be convincing. Today as a result of the break through in computer technology, (which has been successfully applied in the area of seismic exploration), extensive calculations are economically feasible and data quality are controlled easily. Data processing has changed seismic exploration so much that the changes are referred to as digital revolution. Most seismic recording is now done in digital form and most data are now subjected to data processing before being interpreted, (Telford et al., 1976).

Data Format, Processing, Interpretation and Presentation are steps necessary to obtain desired results. First arrival times are usually measured from seismic signals in the field and are recorded in field logs and plots. Traveltime/distance (T/D) plots permit calculation of layer parameters. The results were then interpreted to yield a geologic section of the subsurface. The processing procedure begins with the determination of the first arrival time to each geophone. The enhancement technique was employed to aid in recognizing the first arrivals on the display. Multi-channel seismographs can also assist in identifying this first wave by revealing a trend in the composite received signals. Once the arrival times are determined for each geophone, the time/distance plot is constructed. Straight line segments are fitted to linear sections of the plot by least square techniques. The number of segments and their slopes correspond to the number of geologic layers and their velocities. These

TASUED LIBRARY

velocities and critical distances (determined by breaks in the line segments) are used to calculate the depth of the layer. Forward and reverse shot data taken can be used to provide the true velocities, depth, and dip of each layer in the case of dipping layers. Time/distance plots may show abnormal slopes or breaks. Such plots reveal that the subsurface is not composed of homogeneous layers of uniform thickness and velocity. Several types of conditions are recognizable from their characteristic T/D plots. The degree of geologic scatter in the data is also a good indicator of subsurface conditions. Many possible pitfalls exist in the acquisition, processing, and interpretation of seismic data. Solutions are not unique and all interpretations must be based on some assumptions about the site, together with independent information on the geohydrological conditions at the site. Velocity inversions and thin bed cases may not be detected. Dipping bedding can cause considerable error in calculations; therefore, both forward and reverse lines must be used.

4.2 Processing of seismic tomography data

After every fieldwork follows a processing stage which was done in steps to obtain a processed data good enough for interpretation. These different steps would be discussed. The very first thing to do is to download the data from the Mark6 Terraloc by connecting via a Local Area Network (LAN) cable to the computer, the data were saved in a labeled folder named. The next stage of processing was the conversion of the raw data into the Reflex format, using the software for the interpretation of the raw data. A value of 5 was set for "receiver start" in the "import data" menu 120 for the "receiver end", 0 for the shot position and input format "SEG2" were chosen. Under the plot option menu the scaling factor was set to 20 and the clipping factor was set to 10, the "plotoption" was set to wigglemode, the imported data was stored with a name under "filename". The importation

was done by clicking "convert to Reflex", and the data converted to Reflex format and stored under the folder "RAWDATA".

4.2.1 Filtering

The next stage of processing was the application of filtering processes. But before the filtering, the monitor screen had to be spitted into two (the primary and the secondary window), by clicking "horizontal split" from the "plotoption" menu, on the menu bar. The secondary window contains the raw data, while the primary window holds the processed data.

The first filter that was selected was the 1-D filter; under the 1-D filter menu is the "bandpass frequency" filter. The upper cut off frequency and the lower cut off frequency were set to 150Hz and 5Hz respectively. Afterward, the "ProcessingLabel" was entered and (the processing label must be different from that of the primary file because original and filtered datafile must not have the same filename) and clicking "Start" initiated the filtering process, and the filtered data was placed in the primary window. To allow for the next stage of filtering, the filtered data in the primary window was transferred to the secondary window, by making use of "Change primary to secondary" button on the file menu.

The next stage of processing is the application of gain, to enhance the data quality. The gain is applied under the processing/gain menu. Clicking on gain, within the Gain window, activates the option "manual gain (y)". A table appears on the right side for entering the gain values together with a new window, which allows for interactively entering of the gain values.

KASHIM IBRAHIM LIBRARY

On entering the wanted "Processing Label" and clicking the "start" command, the manual gain processing begins. Again the processing label must be different from that of the primary file. The manual gain (y) corrected data was plotted into the secondary window. In order to use the filtered data set for the next desired filter step, the option "Change Secondary To Primary" was activated having closed the gain window. The gain process was repeated for weaker signals.

4.2.2 Picking First Arrivals

It is easier to pick the first arrivals in a processed data than in the raw data, because the direct and the refracted arrivals are well outlined. With the pick option activated, first arrivals can be picked from the record. The instrument provides a choice between manual picking, continuous pick and a semi- automatic picking using a "phase follower". Using manual pick, with the option "Set Pick" activated, a pick can be set with the left mouse button. The same applies to the manual removal or change of an existing pick after selecting the options "remove" or "change", respectively. Here, those picks are removed or changed which are next to the current cursor position. The right mouse button allows one to toggle between the options "set" and "change". The manual picking of phases is superior to the automatic picking in respect of time consumption for small data sets and in respect of accuracy for data sets of bad quality. For large data sets it is recommended to have a desired phase semi-automatically picked first and then to check the quality of the automatically set picks and corrects them manually if necessary. The picks can be saved with an arbitrary name or automatically if "automaticname" is activated and reloaded any time using the option save and load pick. When saving the pick use the option "ReflexWin" and "2Dtomography" so that the saved pick would be made available during

tomography generation. The picked values can also be manually used to plot the forward and the reverse time curve for depth and velocity determination.

4.2.3. Assigning the picked travel times into layers

Enter the module "traveltime analysis 2D", Load the wanted traveltimes that shall be interpreted together using the option "file/ load traveltimes". Choose all wanted picked files, which shall be interpreted together making multiple choices using the shift key.

Use the option "Edit/ Insert ShotzeroTraveltime" in order to insert a zero traveltime at all shot points if this zero traveltime is not still defined. This is useful in order to better determine the velocities of the uppermost layer. Enter a filename for the actually put together traveltimes and save them on disk. Increase the layer number to 1. Activate the option "assign" in order to assign the wanted traveltimes to layer 1. Assign the traveltimes to layer 1 by using the different possibilities. The traveltimes assigned to layer 1 will be highlighted (default colour green), save the traveltimes. Activate the option "combine" in order to do the inversion for the first layer. The inversion for the first layer only consists of the determination of the velocity.

Activating the option "wavefront- inversion" and a new window opens (the Modeling window) and a model will automatically be created consisting of one layer with the velocities taken from the linear regression analysis of the assigned traveltimes. Some changes of the model could be effected (e.g. remove some unwanted velocity points). Enter a model file name and save this model on disk and close the modeling window. Increase the "layer number" to 2, Activate the option "assign" in order to assign the wanted traveltimes to layer 2. Assign the traveltimes to layer 2 by using the different

KASHIM IBRAHIM LIBRARY

possibilities. The traveltimes assigned to layer 2 will be highlighted (default colour blue). Activate the option "combine" in order to do the inversion for the second layer, enter the forward and the reverse shot numbers - these numbers define the range for doing the inversion of the actual layer. Activate the option "generate". When the option autocombine is chosen a complete combined traveltimecurve (forward and reverse) is generated and the total forward and reverse traveltimes are shown. If total forward and reverse traveltimes difference is more than 5 ms, activate the option "balance" in order to balance the forward and reverse traveltime branches. Activate the option "wavefront-inversion", a file choice window opens, in order to choose the model file containing the first layer already interpreted. The chosen model file is shown within the modeling window. Enter the wanted increment "DeltaX" for the wavefront inversion (e. g. 0.5), start the wavefront- inversion using the option "start".

The new layer boundary is plotted into the model. Extrapolate the inverted boundary to the model borders using the option "horizontal interpolate or Extrapolate", and do some changes of the model if necessary. Save the model using the old or new filename. Close the modeling menu. Repeat the previous steps for layer 3 and so on.

4.3 Performing the refraction tomography

Activate the option "Tomo" The "TomographyGroupBox" opens. Within this group box, enter the necessary tomography parameters. Load the data using the option "load data". Enter the wanted "space increment" (equal in x- and z-direction). Normally this increment should be small enough in order to allow small-scale variations with depth. It may be significantly smaller than the receiver increment. The following options must be set for the refraction tomography: activate the option "curved ray". Set the parameter "start curved

ray" to 1. Enter a quite large value for "max.def.change (%)", e.g. 200 %. Often it is useful to force the first iteration by activating the (option "force 1.iteration") to generate a new model even if the resulting residuals are larger than for the starting model. Enter a smoothing value in x-direction (parameter "average x", e.g. 10). Activate the option "show result" in order to display the tomography model after iteration process. Enter a name for the final model and save. Note; do not use the same name like that of the starting model.

"Start" the tomography. The tomographic result is stored using the "normal" REFLEXW format. Display the result within the 2D-dataanalysis. (Sandmeier, 2003).

4.4 Interpretation

The interpretation of seismic data, involves its expression in geological terms. When competently carried out, it requires the fitting together of all pertinent geological and geophysical information into an integrated picture that is more complete and more reliable than either source is likely to give alone. Ideally, this integration would be accomplished most efficiently if it were done by a single person highly competent both in geophysics and geology. In actual practice, individuals with adequate training and experience in both fields are very few and it is usually necessary for a geophysicist and a geologist to collaborate at this stage of interpretation. (Dobrin, 1976)

4.4.1 Data Interpretation

The travel time curves of the profiles were plotted for the direct and refracted waves, to determine the velocities of the various layers. From the travel time plot it was obvious that most of the profiles have a dipping layer as observed in the intercept times and in the slope of the refractor. As a guide to the seismic Tomography, it is necessary to determine the

48627

RECEIVED
IBRAHIM LIBRARY

thickness of the overburden and the depth to basement, using the following formulas shown below.

$$d = \frac{1}{2} x_{cr} \sqrt{\frac{v_2 - v_1}{v_2 + v_1}}$$

$$d = \frac{1}{2} t_i \frac{v_2 v_1}{\sqrt{v_2^{\,2} - v_1^{\,2}}}$$

$$z_d = \frac{v_1 t_{id}}{2 \cos ic}$$

$$z_u = \frac{v_1 t_{iu}}{2 \cos ic}$$

$$d_u = \frac{d_B}{\cos \theta}$$

$$d_d = \frac{d_A}{\cos \theta}$$

Where v_1 is the velocity of the first layer

v_2 is the velocity of the second layer

x_{cr} is the critical distance

t_i is the intercept time

z_d is the perpendicular distance at the down dip end of spread

z_u is the perpendicular distance at the up dip end of spread

d_u is the thickness of the overburden at the up dip side

d_d is the thickness of the overburden at the down dip side

i_c is the critical angle of incident

θ is the angle of dip.

From the forward and reversed travel time curve plotted for the various profiles, the thickness of the overburden, the velocity of the overburden, and the velocity of the refractor were determined. It is important to note that each profile was sited with the borehole at the center of the profile. Each site contains two profiles i.e. site 1 - profiles 1 and 2, site 2 - profiles 3 and 4, site 3 – profiles 5 and 6, site 4 – profiles 7 and 8.

The first site is located at the Akenzua Hall (Postgraduate hostel). The 1st profile (Figure 4.1) was sited behind the Benin Block in the hostel, with the profile running in the north-south direction. It is a slightly dipping layer. The over burden velocity was estimated to be 841m/s and the refractor velocity, 2087m/s. the thickness of the over burden was estimated to be 10.06m.

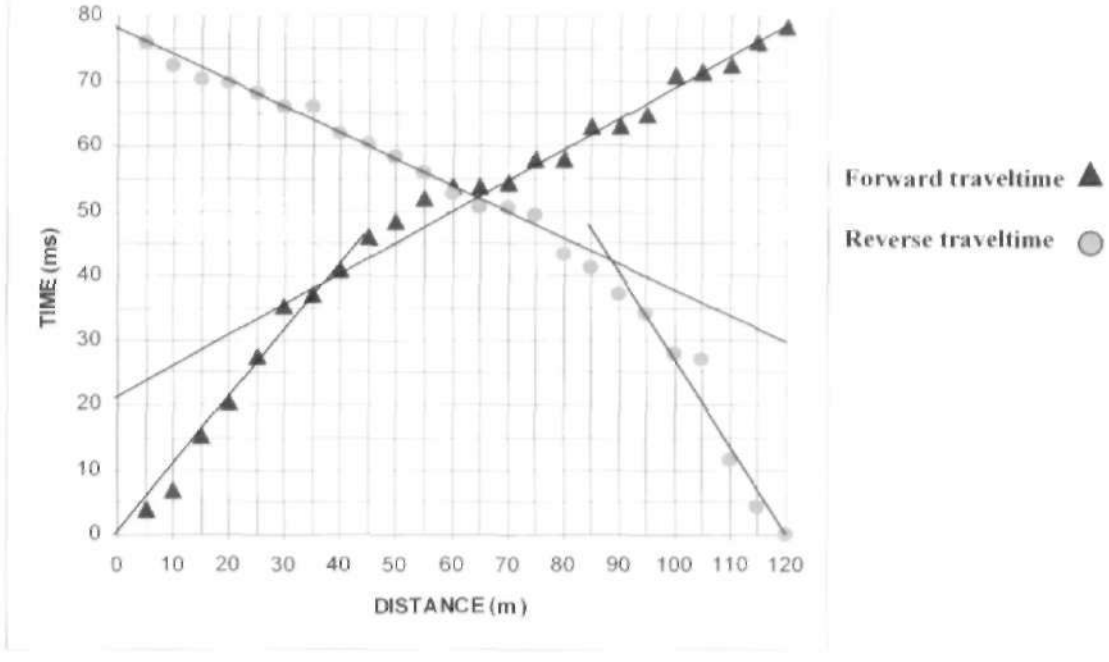


Figure 4.1: Travel time plot for profile 1

The 2nd profile (Figure 4.2) is extends from Ife block through Kano block and the Akenzua Mosque. The profile is dipping in the eastern direction of the profile line. The overburden velocity was estimated to be 784m/s, which is an average of the forward and the reverse profile. The up dip refractor velocity was estimated to be 2798m/s, while the down dip refraction velocity was estimated to be 1876 m/s. The thickness of the overburden at the up dip was estimated to be 16.34m while the down dip was determined to be 7.35m.

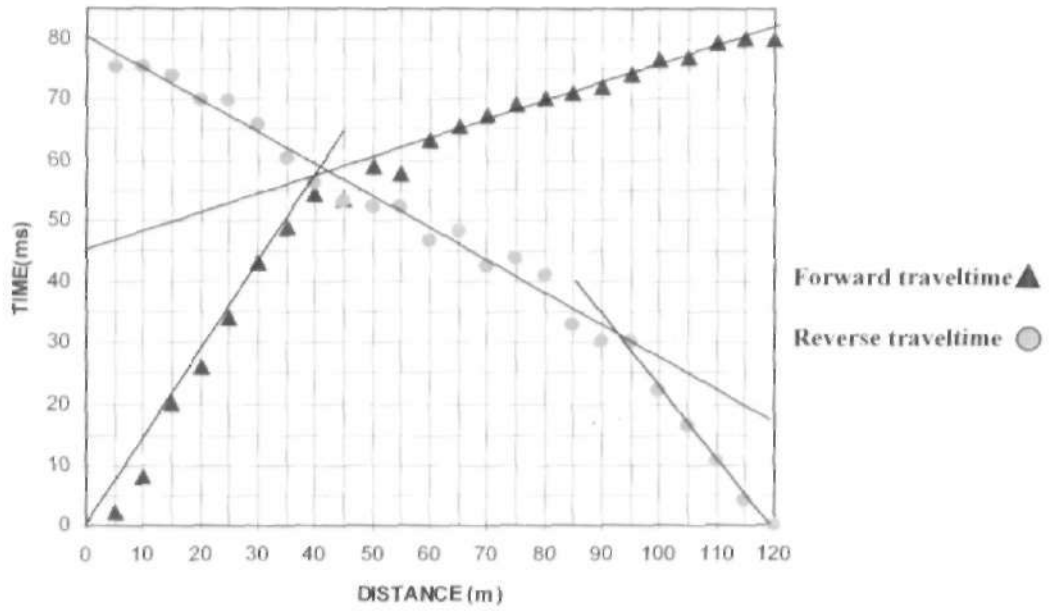


Figure 4.2: Travel time plot for profile 2

The second site is located at the Amina hostel (Girls hostel). The 3rd Profile (Figure 4.3) extends from block 9 through the common room into the main Mosque, in the east-west direction. The profile has a dipping layer in the eastern direction. The overburden velocity was estimated to be 879 m/s, an average from the forward and reverse profile. The refractor velocity at the up dip was estimated to be 2966 m/s and at the down dip it was estimated to be 2509 m/s. The thickness of the overburden was determined to be 14.7 m

from the shot point (up dip) and from the down dip 8.3m. Figure 4.1 show the travel time curves for the direct and refracted rays.

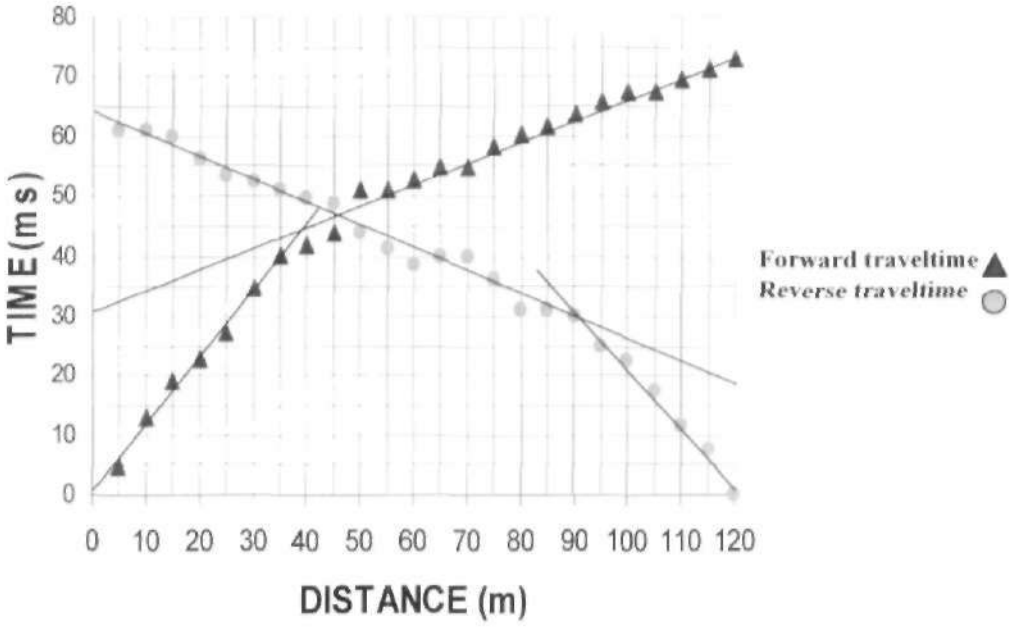


Figure 4.3: Travel time plot for profile 3

The 4th Profile (Figure 4.4) is at the second borehole located just behind the Amina Hall cafeteria (behind block 6 and close to the back gate entrance) it has a dipping layer, in the eastern direction. The velocity of the overburden was estimated to be 935 m/s by averaging both the forward and reversed profile. The up dip refractor velocity was estimated to be 2343 m/s, and the down dip refractor velocity was estimated to be 2094 m/s. The thickness of the overburden from the shot point at the up dip side was estimated at 11.22 m, and thickness of the overburden from the shot point at on the down dip side is about 8.16 m.

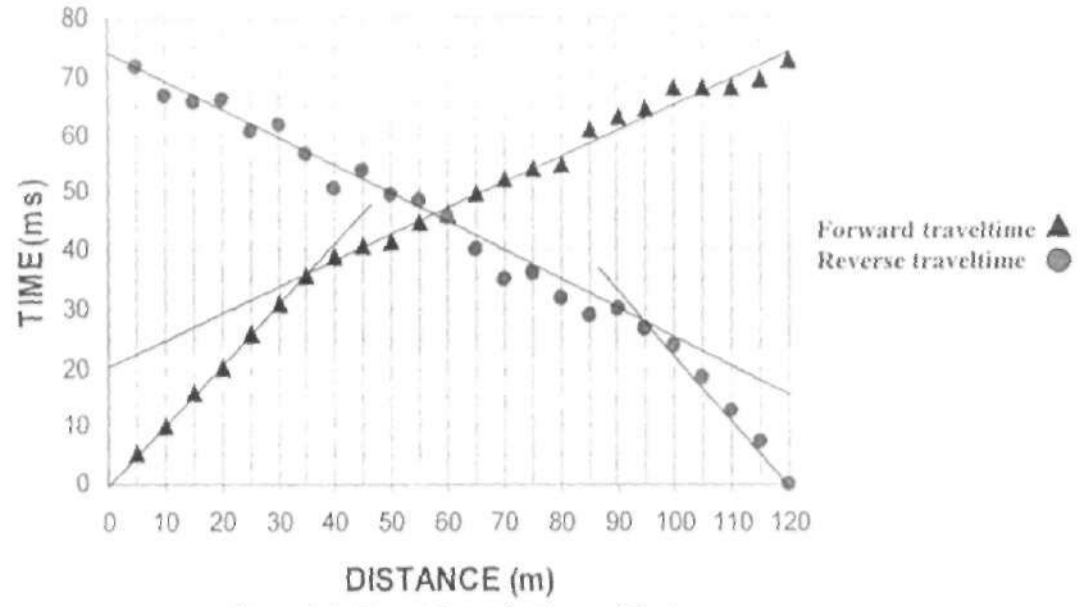


Figure 4.4: Travel time plot for profile 4

The third site was located at the Ribadu/Alexandra Hall (Girls Hostel). The 5th profile (Figure 4.5) was located behind Lb close to the small student Mosque where the borehole is sited. It shows a dipping layer. The overburden velocity was estimated to be 1126m/s and the refractor velocity was estimated to be 2641m/s. the thickness of the overburden was determined to be 11.92m.

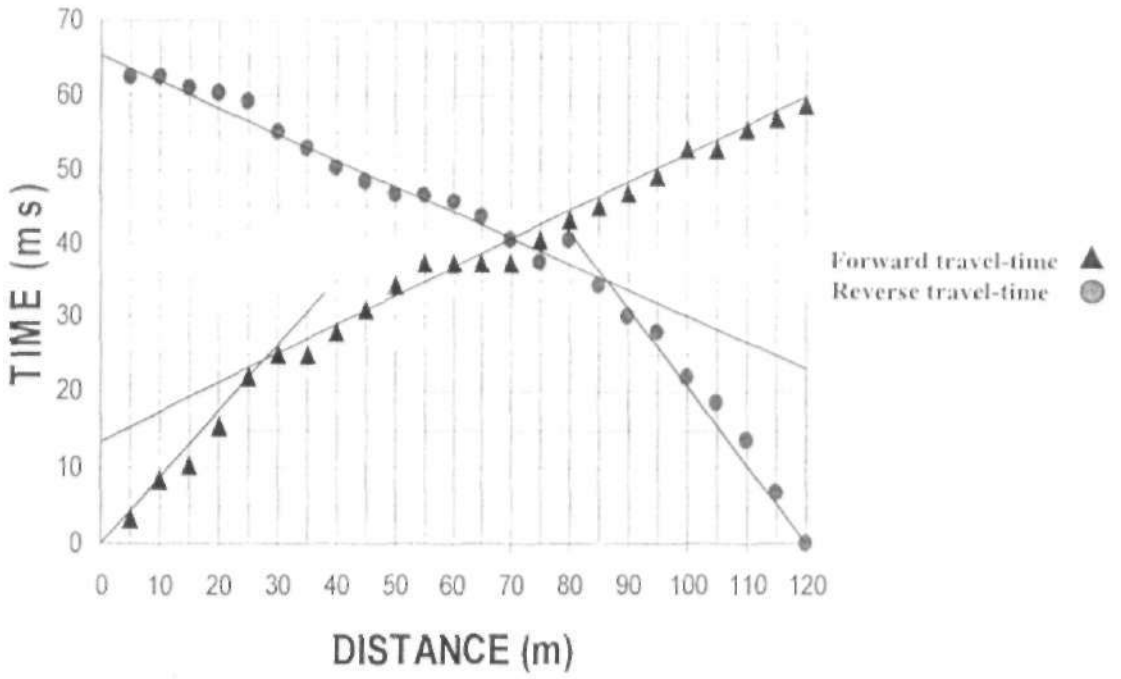


Figure 4.5: Travel time plot for profile 5

The 6th profile (Figure 4.6) was sited behind the Ld block. The profile, taken along the east-west direction shows a slightly dipping layer. The overburden velocity was estimated to be 1049m/s. The velocity of the refractor was estimated at 2666 m/s. The thickness of the overburden was determined to be 10.27m.

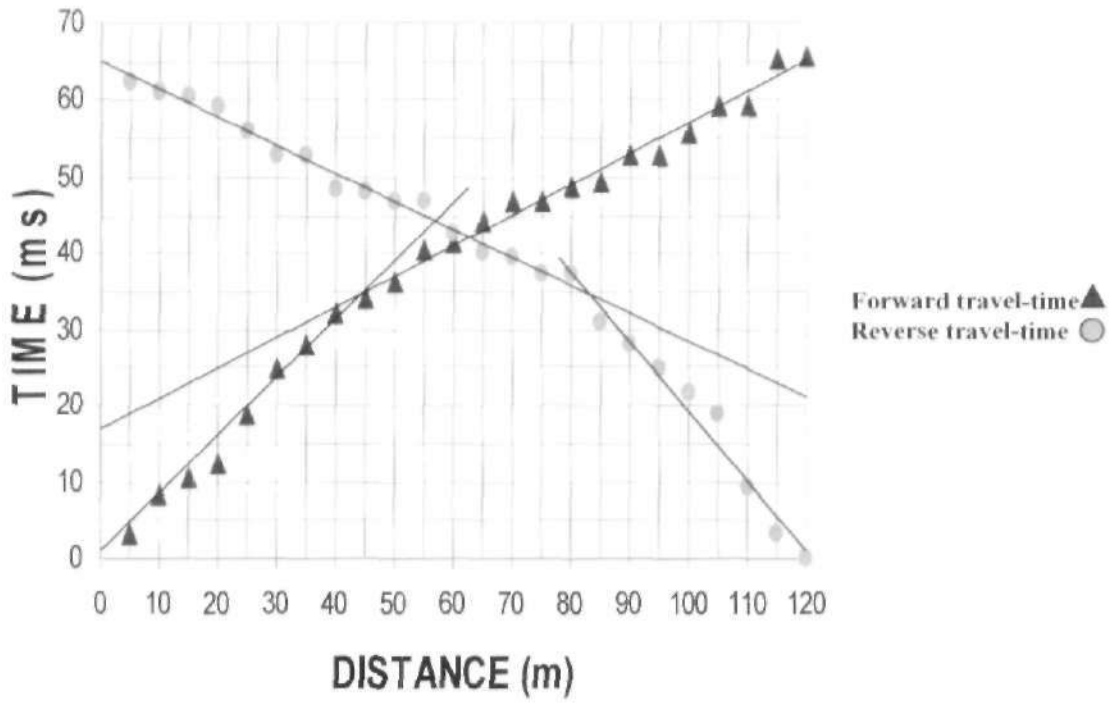


Figure 4.6: Travel time plot for profile 6

The fourth site is located at the Suleiman Hall hostel (Male hostel). The 7th profile (Figure 4.7) extends from the transformer house through blocks 5A and 6A, pointing in the east-west direction. The overburden velocity was determined to be 930m/s, and the refractor velocity was determined to be 2977m/s. the thickness of the overburden was determined to be 9.44m.

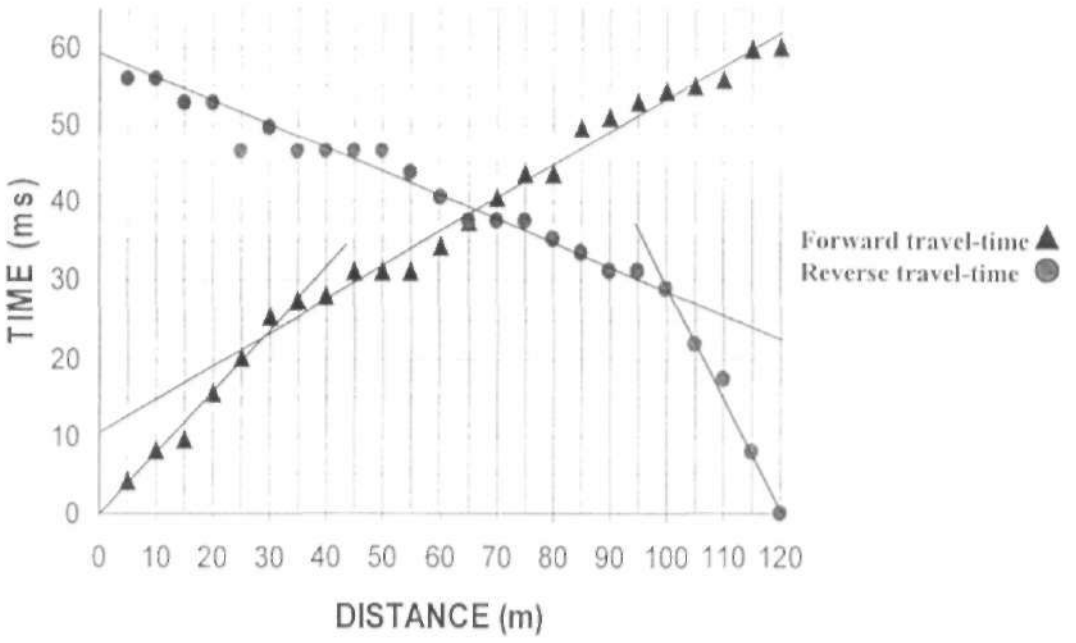


Figure 4.7: Travel time plot for profile 7

The 8th profile (fig. 4.8) was sited beside the F's and A's blocks, extending from the A block common room through blocks A5, A6, A7, F6, F4 to block F2. The profile line is in the north-south direction. The overburden velocity was determined to be 1131m/s, while the refractor velocity was determined to be 2212m/s. the thickness of the overburden was determined to be 8.94m.

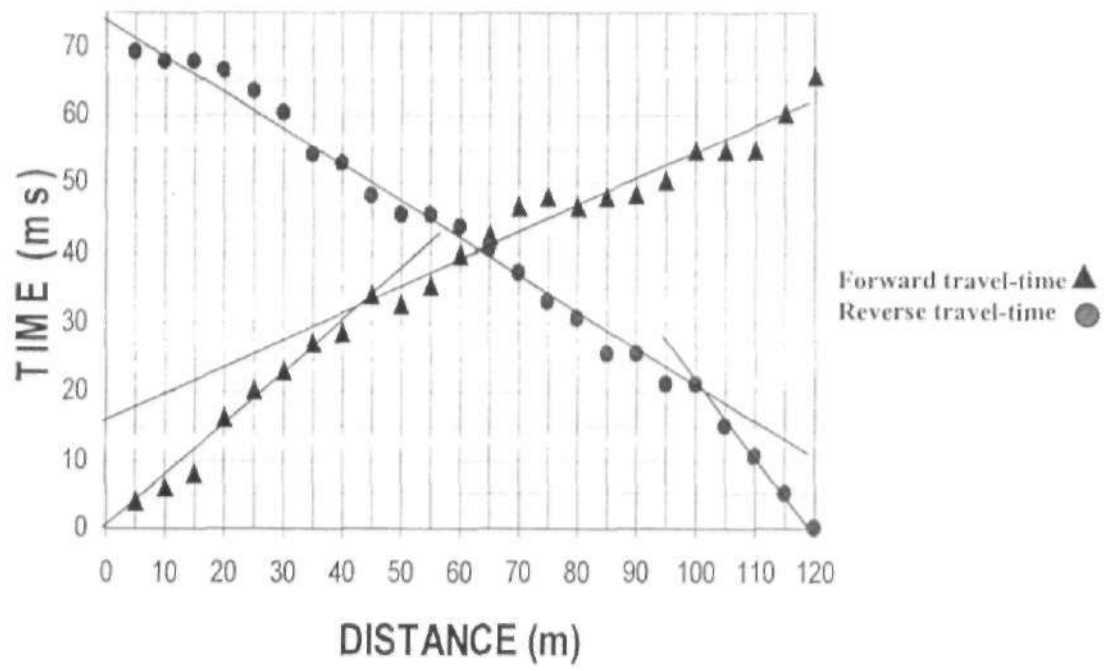


Figure 4.8: Travel time plot for profile 8

Finally, from the results obtained so far, one can conclusively say that the average thickness of the overburden within the survey areas is about 13.7 m, and that the survey area is characterized by dipping layers, in the direction of West to East of the survey area.

4.5 Interpretation of the tomography section

The Tomography section is the colour image of the earth's structure, with each colour representing a range of velocity, characterized by the rainbow colours (blue, light green, yellow, orange, red, indigo to purple colour). Each Tomography section has a colour bar code of velocity range, corresponding with the velocities of the respective layers.

A close examination of each of the Tomography section around each of the borehole sited in the hostels will be discussed in detail.

The first tomographic section (Figure 4.9) located at the Akenzua hostel, indicates that, a particular section shown in blue at the centre of the spread, starting from a depth of about

0.0 to 10.0m, having a velocity range of 648 m/s to 1108 m/s, represent the overburden, which includes the top surface soil (sand clay and laterite) and has a standard velocity range of 350 m/s to 1200 m/s (Table 4.9). This correlates exactly with the borehole log (Table 4.1) that was located exactly at the center of the spread, with a lithology of reddish brown Top soil (between 0.0 to 5.0m) and reddish brown Sandy soil at a depth of about 5.0m to 9.0 m, as overburden layer.

The next layer which starts at a depth of about 10.0 m to a depth of about 24.0m, with a velocity range of 1262 m/s to 2640 m/s, represents a weathered basement which has extended into the Fresh Basement. This layer is made up of saturated sand and clay. It has a standard velocity range of 1500 m/s to 2000 m/s and also correlates exactly with the borehole log (Table 4.1) which has a lithology of Grayish brown sandy clay (3.0m), Mottled clay (5.0m) and Coarse to Medium grain sand (5.0m) as weathered layer (9.0m to 22.0m).

The Fresh Basement starts at a depth of 24.0 m based on the high velocity ranging from about 2640 m/s to 3099 m/s and above. This also agrees with the borehole log, which has a lithology of probably quartzite occurring with gneiss and fresh crystalline rock from a depth of 22.0 m and above.

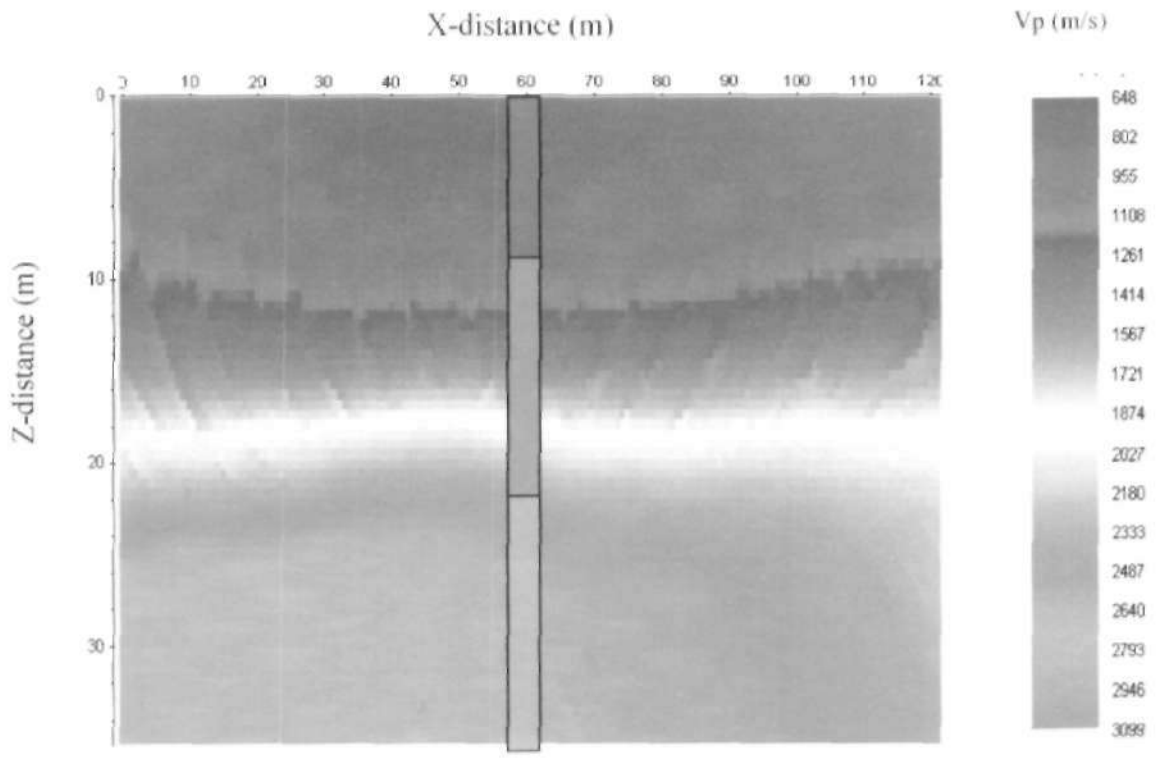


Figure 4.9: Tomographic Section of profile 1- Akenzua Hostel.

Borehole log 1 - Akenzua

Reddish brown topsoil and sandy clay. 0m to 9.0m deep.	Grayish brown sandy clay, Mottled clay, Coarse/Medium grayish sand. 9.0m to 22.0m deep.	Fractured Basement. 22.0m to 27.0m deep.

Table 4.1: Lithology, Aquifer and Geologic section of borehole 1 – Akenzua Hostel (Hydro-Skill Ltd., 2006)

DEPTH (m)		THICKNESS (m)	LAYER DEPTH (m)	INTERPRETED LITHOLOGY	HYDROLOGICAL CHARACTERISTICS
FROM	TO				
0.0	5.0	5.0	Overburden 0.0 – 9.0	Reddish brown topsoil.	
5.0	9.0	4.0		Reddish brown sandy clay	
9.0	12.0	3.0	Weathered basement 9.0 – 22.0	Grayish brown sandy clay	
12.0	17.0	5.0		Mottled clay	
17.0	22.0	5.0		Coarse to Medium grained sand	Aquifer
22.0	27.0	5.0	Fresh Basement 22.0 – 27.0	Fractured basement	Aquifer

The second layer, represented by three colours (green, yellow and red), is the weathered basement, which extends from a depth of about 8.0m to a depth of about 25.0m, with velocity range of 1161 m/s to 2176 m/s. The borehole log shows a lithology of grayish brown sandy clay (2.0m), mottled clay (5.0m) and coarse to medium grained sand (3.0m) as weathered basement from a depth of 8.0m to 18m.

The fresh basement is outlined in the model; it starts at a depth of 25.0 m and continues downward. The borehole log shows a close correlates with fresh basement starting from a depth of about 18.0m to 27.0m and above, Table 4.2.

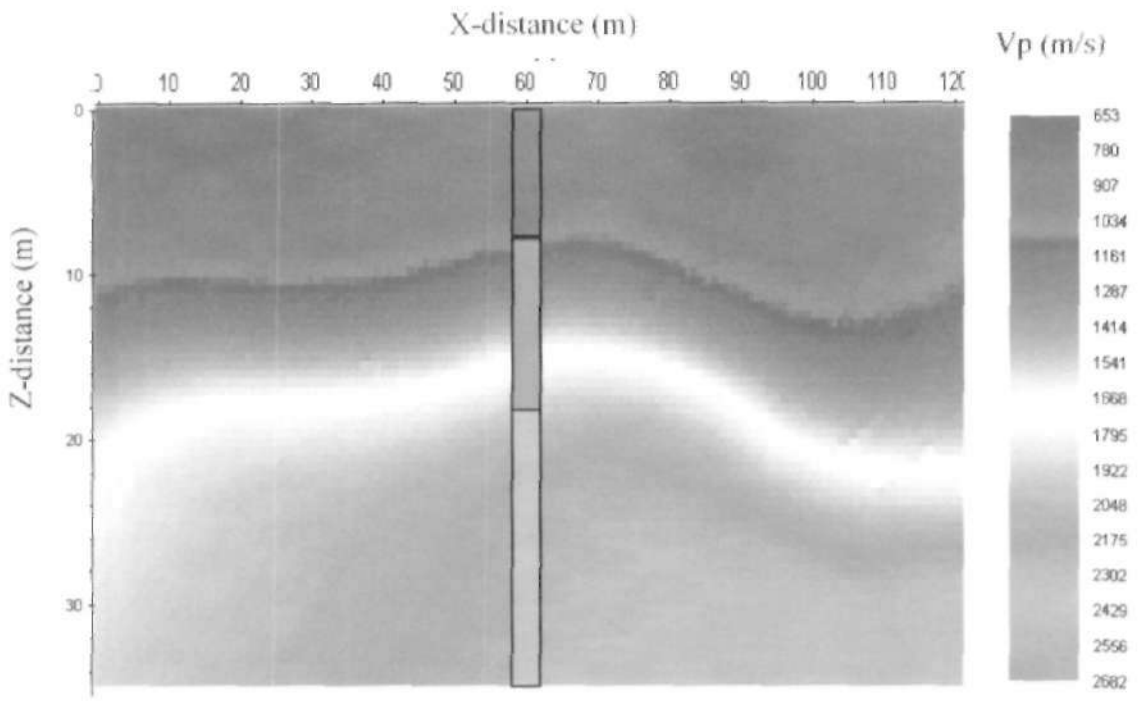


Figure 4.10: Tomographic Section of profile 2- Akenzua Hostel

Borehole log 2 - Akenzua

Reddish brown topsoil and sandy clay. 0m to 8.0m deep.	Grayish brown sandy clay, Mottled clay, Coarse/Medium grayish sand. 8.0m to 18.0m deep.	Fractured Basement. 18.0m to 27.0m deep.

Table 4.2: Lithology, Aquifer and Geologic Section of Borehole 2- Akenzua Hostel (Hydro-Skill Ltd., 2006)

DEPTH (m)		THICKNESS (m)	LAYER DEPTH (m)	INTERPRETED LITHOLOGY	HYDROLOGICAL CHARACTERISTICS
FROM	TO				
0.0	3.0	3.0	Overburden 0.0 – 8.0	Reddish brown topsoil.	
3.0	8.0	5.0		Reddish brown sandy clay	
8.0	10.0	2.0		Grayish brown sandy clay	
10.0	15.0	5.0		Mottled clay	
15.0	18.0	3.0	Weathered basement 8.0 – 18.0	Coarse to Medium grained sand	Aquifer
18.0	27.0	9.0	Fresh Basement 18.0 – 27.0	Fractured basement	Aquifer

The next site is located at the Amina hostel. Figure 4.12 shows the Tomography of profile 3, which extends from block 9 into the Mosque. The blue colour in the section represent the overburden. It extends from 0.0m to about 10.0m, with velocity range of 661 m/s to 1162 m/s. This correlates with the borehole located at the center of the spread whose lithology consists of reddish brown top soil (4.0m) and reddish brown sandy clay (3.0m) as the overburden (7.0m thick) Table 4.3.

The next layer consisting of the green, yellow and red colour codes, start from about 10.0m to 22.0m, it has a velocity range of 1328 m/s to 2004 m/s. This layer is made up of saturated sand, representing the weathered basement, which has extended far into the fresh basement as shown in figure 4.11. This correlates with the borehole, table 4.3.

Although the fresh basement is not continuous from a depth of about 22.0m and above, it appears like an out-crop at one end of the spread. It has a velocity range is from 2831m/s to 3331m/s and above. This correlates with the borehole log. Table 4.3

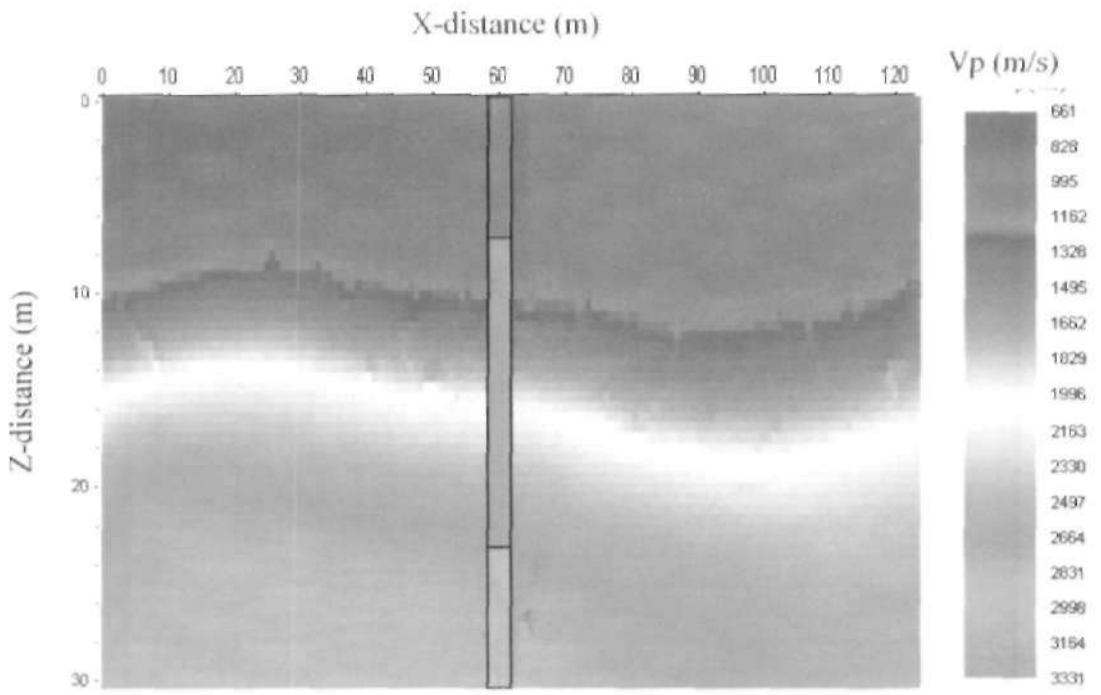


Figure 4.11: Tomographic Section of profile 3 - Amina Hostel

Borehole Log 1 – Amina Hostel

Reddish brown topsoil and sandy clay. 0m to 7.0m deep.	Grayish brown sandy clay, Fine to Medium grain sand, Coarse grain sand, Medium grain sand. 7.0m to 23.0m deep.	Fractured Basement. 23.0m to 30.0m deep.

Table 4.3: Lithology, Aquifer and Geologic Section of Borehole 1-Amina Hostel (Hydro-Skill Ltd., 2006)

DEPTH (m) FROM	TO	THICKNESS (m)	LAYER DEPTH (m)	INTERPRETED LITHOLOGY	HYDROLOGICAL CHARACTERISTICS
0.0	4.0	4.0	Overburden 0.0 – 7.0	Reddish brown topsoil.	
4.0	7.0	3.0		Reddish brown sandy clay	
7.0	10.0	3.0	Weathered basement 7.0 – 23.0	Grayish brown sandy clay	
10.0	14.0	4.0		Fine to Medium grained sand	Aquifer
14.0	17.0	3.0		Coarse grained sand	Aquifer
17.0	23.0	6.0		Medium grained sand	Aquifer
23.0	30.0	7.0	Fresh Basement 23.0 – 30.0	Fractured basement	Aquifer

The Tomographic section (Figure 4.12) of profile 4 (starting from the block 6 to the cafeteria) in the Amina Hostel shows an overburden (representing the blue colour) of mainly sandy clay up to a depth of about 6.0m at the end of the profile and about 10.0m at the start of the profile. The velocity of the overburden is between 758m/s to 1248m/s. This correlates with the borehole log (Table 4.4) with lithology of reddish brown top soil (6.0m) and reddish brown sandy clay (2.0m) as overburden (8.0m thick).

The next layer starts from a depth of about 6.0m to 24.0m at the end of the profile and from 10.0m and above at the start of the profile, with velocity range of 1411m/s to 2717m/s. This weathered layer extends far into the basement (a sign of dipping layer) and is made up of the saturated sand. This correlates with the borehole log (table 4.4) with lithology of grayish brown sandy clay (4.0m), Fine to Medium grain sand (2.0m), Coarse grain sand (2.0m) and Medium grain sand (9.0m), representing the weathered basement (8.0m to 30.0m).

The fresh basement appears like an out-crop towards the end of the profile, from a depth of about 30.0m, with velocity range from 2880m/s to 3300m/s and above. This velocity shows a probably of having Gneiss and Schist as basement.

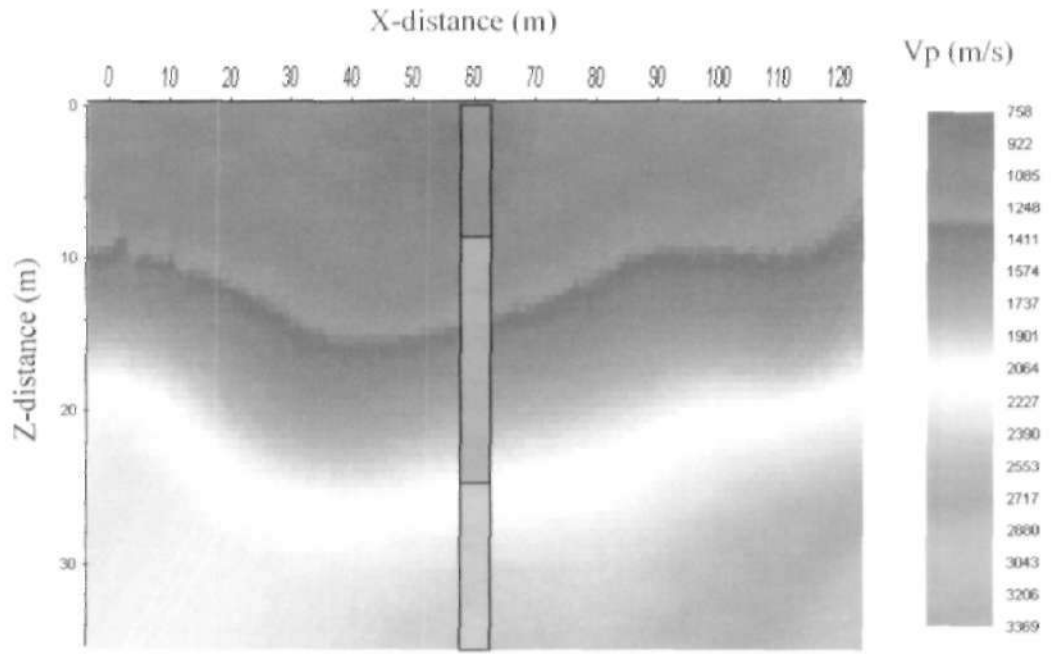


Figure 4.12: Tomographic Section of profile 4 – Amina Hostel

Borehole Log 2 – Amina Hostel

Reddish brown topsoil and sandy clay. 0m to 8.0m deep.	Grayish brown sandy clay, Fine to Medium grain sand, Coarse grain sand, Medium grain sand. 8.0m to 25.0m deep.	Fractured Basement. 25.0m to 37.0m deep.

KAMUZU LIBRARY

Table 4.4: Lithology, Aquifer and Geologic Section of Borehole 2 – Amina Hostel (Hydro-Skill Ltd., 2006)

DEPTH (m)		THICKNESS (m)	LAYER DEPTH (m)	INTERPRETED LITHOLOGY	HYDROLOGICAL CHARACTERISTICS
FROM	TO				
0.0	6.0	6.0	Overburden 0.0 – 8.0	Reddish brown topsoil.	
6.0	8.0	2.0		Reddish brown sandy clay	
8.0	12.0	4.0	Weathered basement 8.0 – 25.0	Grayish brown sandy clay	
12.0	14.0	2.0		Fine to Medium grained sand	
14.0	16.0	2.0		Coarse grained sand	Aquifer
16.0	25.0	9.0		Medium grained sand	Aquifer
25.0	37.0	12.0	Fresh Basement 25.0 – 37.0	Fractured basement	Aquifer

The next site is the Ribadu hostel. Figure 4.13 shows the Tomographic section of the 5th profile behind the Lc block. The blue colour represent the over burden which extends from 0.0m to about 6.0m, with velocity range of 1121m/s to 1439m/s. This correlate with the borehole log (Table 4.5) located at the center of the spread, with lithology of reddish brown top soil (3.0m) and reddish brown sandy clay (2.0m) as overburden (5.0m thick).

The next layer (contains the green, yellow and red colours) starts from a depth of about 6.0m to about 25.0m and has velocity range from 1545m/s to 2393m/s. These represent the weathered basement made up of saturated sand. This correlates to a certain depth with the borehole log whose lithology consist of Grayish brown sandy clay (3.0m), Fine to Medium grained sand (2.0m), Coarse grained sand (5.0m) and Medium grained sand (10.0m) as weathered basement (20.0m thick) Table 4.5.

The third layer containing the purple colour represent the fresh basement (probably of Gneiss or Schist), which starts from a depth of about 25.0m and above and has a velocity range of 2393m/s to 2817m/s and above. This correlates with the borehole log with a lithology of fractured basement Table 4.5.

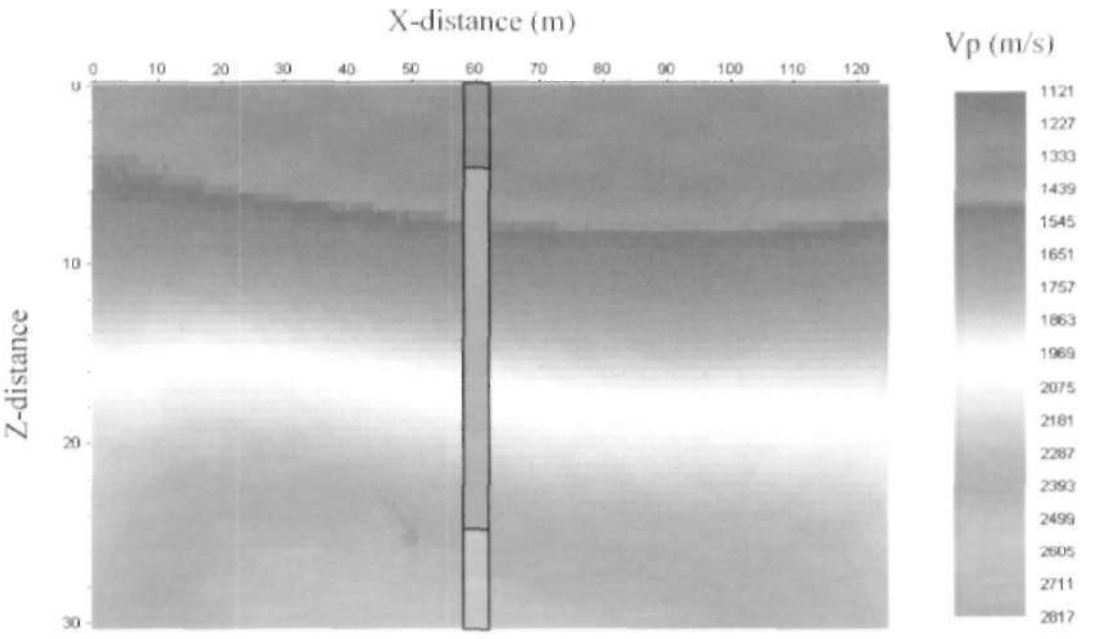


Figure 4.13: Tomographic Section of profile 5 – Ribadu Hostel

Borehole Log 1 – Ribadu Hostel

Reddish brown topsoil and sandy clay. 0m to 5.0m deep.	Grayish brown sandy clay, Fine to Medium grain sand, Coarse grain sand, Medium grain sand. 5.0m to 25.0m deep.	Fractured Basement. 25.0m to 40.0m deep.

KASHIM IBRAHIM LIBRARY

Table 4.5: Lithology, Aquifer and Geologic section of Borehole 1 – Ribadu Hostel (Hydro-Skill Ltd., 2006)

DEPTH (m)		THICKNESS (m)	LAYER DEPTH (m)	INTERPRETED LITHOLOGY	HYDROLOGICAL CHARACTERISTICS
FROM	TO				
0.0	3.0	3.0	Overburden 0.0 – 5.0	Reddish brown topsoil.	
3.0	5.0	2.0		Reddish brown sandy clay	
5.0	8.0	3.0	Weathered basement 5.0 – 25.0	Grayish brown sandy clay	
8.0	10.0	2.0		Fine to Medium grained sand	
10.0	15.0	5.0		Coarse grained sand	Aquifer
15.0	25.0	10.0		Medium grained sand	Aquifer
25.0	40.0	15.0	Fresh Basement 25.0 – 40.0	Fractured basement	Aquifer

Figure 4.14 shows the Tomography of profile 6 located behind the Ld block. The blue colour section starting from 0.0m to a depth of about 8.0m, with velocity range from 631m/s to 1106m/s, represents the overburden made up of sandy clay. This correlates exactly with borehole log (Table 4.6) located at the center of the spread, with lithology of reddish brown top soil (4.0m) and reddish brown sandy clay (2.0m) as overburden (6.0m thick).

The second layer consisting of the green, yellow and red colours that extend from 8.0m to 18.0m with velocity range from 1264m/s to 2530m/s represent the weathered basement. This layer is made up of the saturated sand and correlates with the borehole log whose lithology consist of the grayish brown sandy clay (4.0m), fine to medium grained sand (4.0m), coarse grained sand (3.0m) and medium grained sand (3.0m) as weathered basement (14.0m thick) Table 4.6.

The purple colour code starting from a depth of about 18.0m and above with velocity range from 2600m/s to 3183m/s represents the fresh basement layer (mainly gneiss or schist). This correlates with the borehole log as the fractured basement.

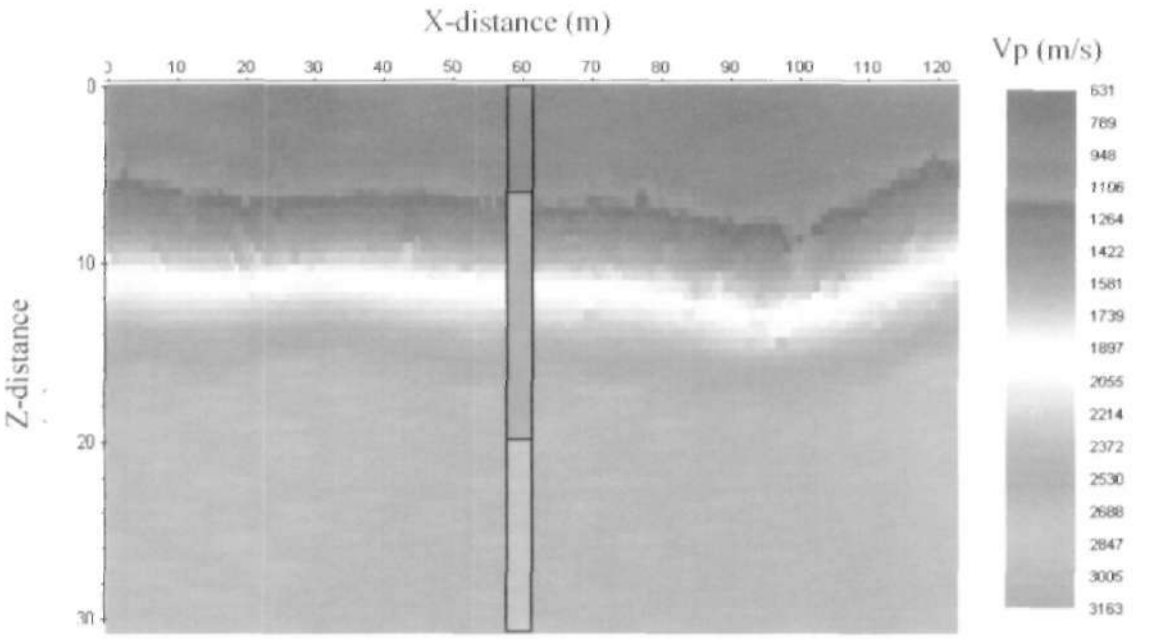


Figure 4.14: Tomographic Section of profile 6 – Ribadu Hostel

Borehole Log 2 – Ribadu Hostel

Reddish brown topsoil and sandy clay. 0m to 6.0m deep.	Grayish brown sandy clay, Fine to Medium grain sand, Coarse grain sand, Medium grain sand. 6.0m to 20.0m deep.	Fractured Basement. 20.0m to 37.0m deep.

Table 4.6: Lithology, Aquifer and Geologic Section of Borehole 2- Ribadu Hostel (Hydro-Skill Ltd., 2006)

DEPTH (m)		THICKNESS (m)	LAYER DEPTH (m)	INTERPRETED LITHOLOGY	HYDROLOGICAL CHARACTERISTICS
FROM	TO				
0.0	4.0	4.0	Overburden 0.0 – 6.0	Reddish brown topsoil.	
4.0	6.0	2.0		Reddish brown sandy clay	
6.0	10.0	4.0	Weathered basement 6.0 – 20.0	Grayish brown sandy clay	
10.0	14.0	4.0		Fine to Medium grained sand	
14.0	17.0	3.0		Coarse to grained sand	Aquifer
17.0	20.0	3.0		Medium grained sand	Aquifer
20.0	37.0	17.0	Fresh Basement 20.0 – 37.0	Fractured basement	Aquifer

The next site is located at the Suleiman Hostel. Fig. 4.15 shows a Tomography of profile 7 located close to the transformer in front of block A4 and extending in between block A5 and A6. The top blue colour section extends from 0.0m to about 12.0m, with velocity range of 951m/s to 1464m/s, representing the overburden (mainly laterite and sandy clay). The borehole log (Table 4.7) situated at the center of the spread correlates. The lithology shows the over burden (0 to 8.0m) consisting of reddish brown top soil (5.0m) and reddish brown sandy clay (3.0m) as overburden (8.0m thick).

The next layer starts from a depth of 12.0m to 26.0m with velocity range from 1464 to 2984m/s represent a layer made up of saturated sand. This layer is the weathered basement. The borehole log shows a weathered basement (from 8.0m to 22.0m) consist of grayish brown sandy clay (3.0m), fine to medium grained sand (4.0m) and coarse grained sand (5.0m) Table 4.7.

The next layer is the purple colour with velocity range from 2984m/s to 3660m/s and depth from 26.0m and above representing the fresh basement. The borehole log shows a fresh basement (from 22.0 to 37.0m) consisting of the fractured basement Table 4.7.

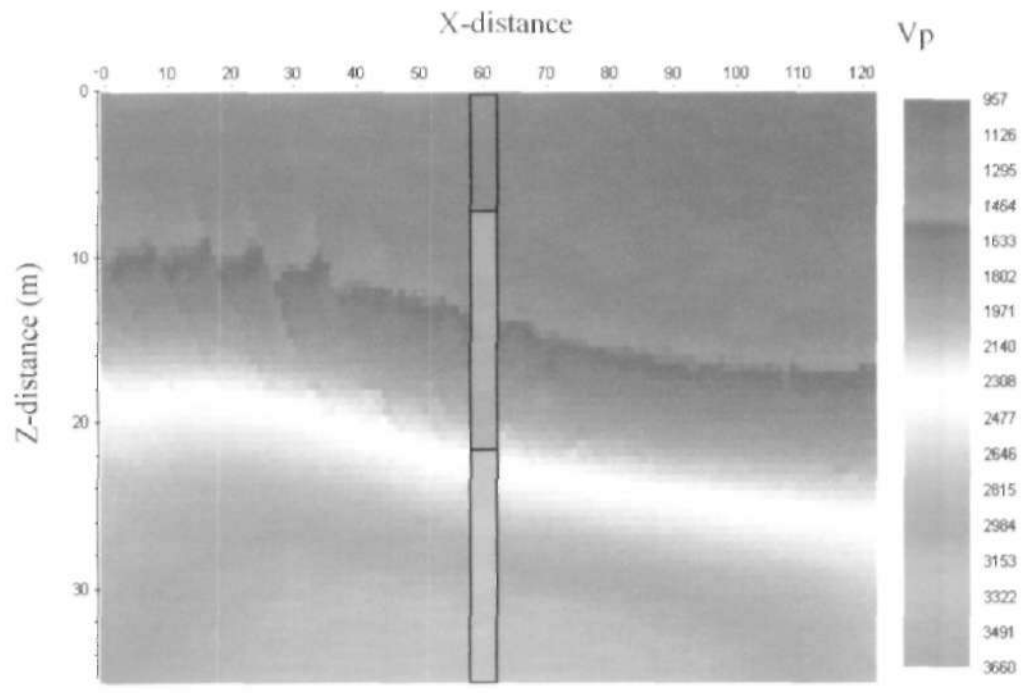


Figure 4.15: Tomographic Section of profile 7- Suleiman Hostel

Borehole Log 1-- Suleiman Hostel

Reddish brown topsoil and sandy clay. 0m to 8.0m deep.	Grayish brown sandy clay, Fine to Medium grain sand, Coarse grain sand. 8.0m to 22.0m deep.	Fractured Basement. 22.0m to 37.0m deep.

KASHMIR INSTITUTE LIBRARY

Table 4.7: Lithology, Aquifer and Geologic Section of Borehole 1 – Suleiman Hostel (Hydro-Skill Ltd., 2006)

DEPTH (m)		THICKNESS (m)	LAYER DEPTH (m)	INTERPRETED LITHOLOGY	HYDROLOGICAL CHARACTERISTICS
FROM	TO				
0.0	5.0	5.0		Reddish brown topsoil.	
5.0	8.0	3.0	Overburden 0.0 – 8.0	Reddish brown sandy clay	
8.0	11.0	3.0		Grayish brown sandy clay	
11.0	15.0	4.0		Fine to Medium grained sand	Aquifer
15.0	22.0	7.0	Weathered basement 8.0 – 22.0	Coarse to grained sand	Aquifer
22.0	37.0	15.0	Fresh Basement 22.0 – 37.0	Fractured basement	Aquifer

Figure 4.16 shows the Tomography of profile 8 located beside F and A blocks, extending from block F2 to block A5. The blue colour starting from 0.0m to depth of about 0.8m with velocity range of 1001m/s to 1442m/s represents the overburden layer consisting of mainly laterite and sandy clay. The borehole log sited at the center of spread, show a close correlation with the lithology of reddish brown top soil (3.0m) and reddish brown sandy clay (4.0m) representing the overburden (0.0m to 7.0m). Table 4.16

The next layer consisting of the green, yellow and red colour starts from a depth of about 0.8m to 26.0m with velocity range of 1442m/s to 2706m/s represent the weathered basement of saturated sand. The lithology of the log shows a grayish brown sandy clay (2.0m), Fine to Medium grained sand (3.0m), Coarse grained sand (8.0m) and Medium grained sand (5.0m), representing the weathered basement (7.0m to 25.0m).

The purple colour code starting from a depth of 26.0m and above with velocity range

2766m/s to 3355m/s, represents the fresh basement, which is probably Schist or Gneiss. This correlates with the log, showing fractured basement (25.0m and above).

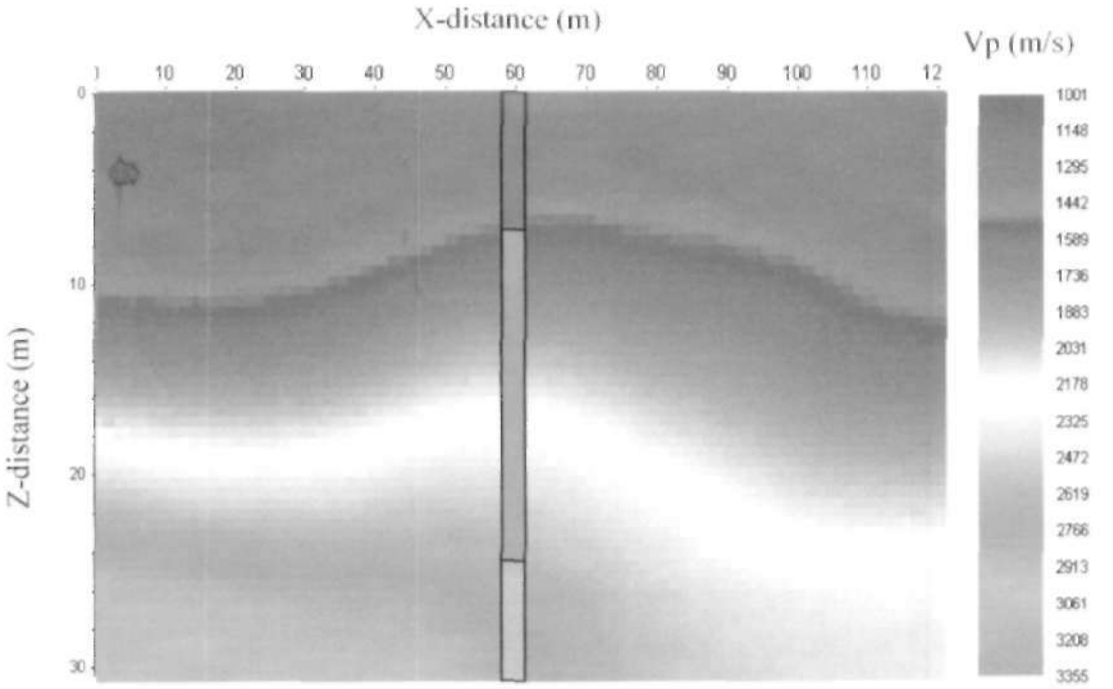


Figure 4.16: Tomography section of profile 8 – Suleiman Hostel

Borehole Log 2 – Suleiman Hostel

Reddish brown topsoil and sandy clay. 0m to 7.0m deep.	Grayish brown sandy clay, Fine to Medium grain sand, Coarse grain sand, Medium grain sand. 7.0m to 25.0m deep.	Fractured Basement. 25.0m to 37.0m deep.

KASHIM IBRAHIM LIBRARY

Table 4.8: Lithology, Aquifer and Geologic Section of Borehole 2- Suleiman Hostel (Hydro-Skill Ltd., 2006)

DEPTH (m)		THICKNESS (m)	LAYER DEPTH (m)	INTERPRETED LITHOLOGY	HYDROLOGICAL CHARACTERISTICS
FROM	TO				
0.0	3.0	3.0	Overburden 0.0 – 7.0	Reddish brown topsoil.	
3.0	7.0	4.0		Reddish brown sandy clay	
7.0	9.0	2.0	Weathered basement 7.0 – 25.0	Grayish brown sandy clay	
9.0	12.0	3.0		Fine to Medium grained sand	
12.0	20.0	8.0		Coarse grained sand	Aquifer
20.0	25.0	5.0		Medium grained sand	Aquifer
25.0	37.0	12.0	Fresh Basement 25.0 – 37.0	Fractured basement	Aquifer

Further deductions can be made from the tomography section. Close observations show that; profiles 1, 2, 3, 4 and 8 are dipping layers in the eastern direction (with the up dip point at the first geophone point and the down dip point at the last geophone position) and profiles 5 and 7 are dipping layers in the western direction (with the down dip point at the first geophone point and the up dip point at the last geophone position). A close examination of the sections shows that the weathered layer extends down into the fresh basement. Some of the tomography sections show thin layers of weathered layer and this implies that the layer cannot support the storage of water. The borehole log shows that all the layers contain clay to about 16% to 20% except for the Akenzua Hostel were the clay or clay mixed soil is above 20%, this clay layer absorbs the water and expands thereby leaving very little amount of water for the next layer. This give reason why any borehole in this area cannot yield water effectively. The cracking and sinking of buildings in the Ribadu and Suleiman Hostels may be due to the poor foundations laid on these clayey

areas. Each profile can be distinction into three layers of overburden (thickness of about 9.0 m), weathered basement (15.0 m thick) and the fresh basement.

The density values of the various layers were calculated from the velocity of each layer which correlates with the density of the rock type of the formation (Kearey et al., 2002, Dobrin, 1976 and Osemeikhian and Asokhia, 1994).

$$\rho = \Lambda v^{0.25}$$

where ρ is the density of the given rock material, v is the velocity of a given layer and Λ is a constant of proportionality.

Table 4.9: Standard Velocity and Density/Calculated Velocity and Density (Kearey et al., 2002; Dobrin, 1976).

Rock type	Standard velocity (m/s)	Corresponding tomography velocity (m/s)	Standard density (kg/m^3)	Density (kg/m^3) base on tomography velocity model	Tomography model depth (m)	Borehole depth (m)	Formation
Sandy clay	900 to 1200	804 to 1272	1630 to 2600	1899 to 2432	0 to 9.0	0 to 7.5	Overburden
Sand (water saturated)	1500 to 2000	1374 to 1883	2120 to 2278	2120 to 2278	9.0 to 24.0	7.5 to 23.0	Weathered basement
Gneisses and schist	2800 to 5500 and above	2438 and above	2500 to 2810	2478	24.0 to 35	23.0 to 35.0	Fresh basement complex

CHAPTER FIVE

SUMMARY, CONCLUSION AND RECOMMENDATION

5.1 Summary of Results

The following are summary of results from the travel time curves, tomography sections and the borehole logs.

(i) The results obtained so far, showed that the average thickness of the overburden within the survey area is about 9.0m, which is a characteristic of the basement complex areas like Zaria.

(ii) It was clear from the tomography section and confirmed by the borehole log, that the depth to the weathered basement is about 9.0 m, and the depth to the fresh basement is about 24.0 m.

(iii) The tomography section revealed that the lithology within the survey area has the surface soil as unconsolidated material made of laterite. This is immediately underlain by sandy clay, which extends to the depth of the weathered basement.

(iv) The weathered basement, which starts at a depth of about 10.0m, contains the aquifer located at a depth of about 13.0m. This was inferred from the velocity range of the water table, which is about 1500m/s to 2000 m/s. The weathered basement extends up to about 10.0m before hitting the fresh basement. The lithology within this region is made up of sand as confirmed by the borehole log to contain grayish brown medium and coarse sand - gravels and pebbles.

(v) The fresh basement which is made up of schist and gneiss, sets in from the depth of 24.0m and extends continuously downwards.

(vii) From the tomography sections, some of the profiles show an undulating basement.

(viii) From the velocity values and the borehole logs, it is observed that the subsurface is composed of about 15% to 40% of clay or clay mixed soil over the studied area.

5.2 Conclusion

From the results obtained so far, the sinking block in the Suleiman hall was due to the high clay content in the vicinity. This method is suitable for detecting the lithology of the subsurface, the fractured zones and depth to basement of the subsurface. One can conclusively say that seismic refraction tomography is an accurate geophysical method that is ideally suited for subsurface investigation, which includes engineering survey, geophysical survey and geological survey.

5.3 Recommendation

It is recommended that more detailed geophysical work be carried out not only in the survey area but also in the whole of campus area to generally determine the lithology within the campus. Also, the use of seismic reflection tomography, which is recommended for a basement terrain, should be explored. The three dimension (3D) reflection tomography, can give a better image of the subsurface. Finally, that a law should be put in place banning the illegal erection of buildings (especially tall buildings like the residential buildings) and sinking of boreholes without carrying out appropriate geophysical investigation of the subsurface.

KASHIM IBRAHIM LIBRARY

REFERENCES

Adetola, S. O. (1999). A detailed study of Teleseismic P-wave travel-time residuals at Ahmadu Bello University, Zaria. M.Sc. Thesis, Department of Physics, A.B.U., Zaria.

Chiemeke, C. C. (2005). Application of Seismic Refraction Tomography in Basawa Area of Zaria. M.Sc. Thesis, Department of Physics, Ahmadu Bello University, Zaria.

Dobrin, M. B. (1976). Introduction to Geophysical Prospecting (3rd Edition), Megraw-Hill, New York, Pp 630.

Eigbefo, C. (1978). Hydrology of the Kubanni Drainage Basin, Zaria. Unpublished M.Sc. thesis, Department of Physics, Ahmadu Bello University, Zaria.

Gregory A., (2002) Application of Tomography, Brookfield Press, Brisbane, Australia, Pp 476.

Hydro Skill Ltd, (2006). Hydrological log of boreholes at students hostels, Ahmadu Bello University, Zaria.

Kearey P., Hill I. and Brooks M. (2002) An Introduction To Geophysical Exploration (Ed). Tj International Ltd., Padstow, Cornwall, United Kingdom. Pp 21 to 122.

Lowrie W. (1997). Fundamental of Geophysics. Cambridge University Press, Pp 354.

McCurry, P. (1970). The Geology of the Zaria Sheet 102 S.W. And its Region. In: Mortimore, M.J. (Ed.). Department of Geography Occasional Paper No.4., Ahmadu Bello University, Zaria.

Ogah A. J., (1990). Application of Beam Forming Techniques to Enhance Low Quality Seismic Refraction Data at the Kubanni Drainage Basin. Unpublished M.Sc Thesis, Department of Physics, Ahmadu Bello University, Zaria.

Osemeikhian J. E. A and Asokhia M. B. (1994). Applied Geophysics, Stamatas Services Ltd.

Sandmeier, K. J. (2003) User's Guide, Manual On Reflex Software.

Telford W. M. Geldart, L. P. Sherriff, R. E and Keys D.A. (1976). Applied Geophysics, Cambridge University Press.

KASHIM IBRAHIM LIBRARY

Tien-when L. and Philip L., (1994), Fundamentals of Seismic Tomography, Society of Exploration Geophysicists.

Yusuf, D. B. 2000, Comparing the effectiveness of the two-electrode array with the symmetrical Schlumberger array over the main campus of Ahmadu Bello University, Zaria. M. Sc. Thesis, Department of Physics, Ahmadu Bello University.

Zhao D. and Kayal J. R. (2000), Impact of Seismic Tomography on earth sciences, Department of Earth Sciences, Ehime University, Matsuyama 790, Japan.